



Accelerated contributions of Canada's Baffin and Bylot Island glaciers to sea level rise over the past half century

A. Gardner^{1,2}, G. Moholdt³, A. Arendt⁴, and B. Wouters⁵

¹Clark Graduate School of Geography, Clark University, Worcester, MA 01610, USA

²Department of Atmospheric, Oceanic and Space Science, University of Michigan, Ann Arbor, MI 48109, USA

³Institute of Geophysics and Planetary Physics, Scripps Institution of Oceanography, La Jolla, CA 92093, USA

⁴Geophysical Institute, University of Alaska, Fairbanks, AK 99775, USA

⁵The Royal Netherlands Meteorological Institute, 3730 AE De Bilt, The Netherlands

Correspondence to: A. Gardner (agardner@clarku.edu)

Received: 12 March 2012 – Published in The Cryosphere Discuss.: 26 April 2012

Revised: 4 September 2012 – Accepted: 5 September 2012 – Published: 12 October 2012

Abstract. Canadian Arctic glaciers have recently contributed large volumes of meltwater to the world's oceans. To place recently observed glacier wastage into a historical perspective and to determine the region's longer-term (~50 years) contribution to sea level, we estimate mass and volume changes for the glaciers of Baffin and Bylot Islands using digital elevation models generated from airborne and satellite stereoscopic imagery and elevation postings from repeat airborne and satellite laser altimetry. In addition, we update existing glacier mass change records from GRACE satellite gravimetry to cover the period from 2003 to 2011. Using this integrated approach, we find that the rate of mass loss from the region's glaciers increased from $11.1 \pm 3.4 \text{ Gt a}^{-1}$ ($271 \pm 84 \text{ kg m}^{-2} \text{ a}^{-1}$) for the period 1963–2006 to $23.8 \pm 6.1 \text{ Gt a}^{-1}$ ($581 \pm 149 \text{ kg m}^{-2} \text{ a}^{-1}$) for the period 2003–2011. The doubling of the rate of mass loss is attributed to higher temperatures in summer with little change in annual precipitation. Through both direct and indirect effects, changes in summer temperatures accounted for 70–98 % of the variance in the rate of mass loss, to which the Barnes Ice Cap was found to be 1.7 times more sensitive than either the Penny Ice Cap or the region's glaciers as a whole. This heightened sensitivity is the result of a glacier hypsometry that is skewed to lower elevations, which are shown to have a higher mass change sensitive to temperature compared to glacier surfaces at higher elevations. Between 2003 and 2011 the glaciers of Baffin and Bylot Islands contributed $0.07 \pm 0.02 \text{ mm a}^{-1}$ to sea level rise accounting for 16 % of the total contribution from glaciers outside of Green-

land and Antarctica, a rate much higher than the longer-term average of $0.03 \pm 0.01 \text{ mm a}^{-1}$ (1963 to 2006).

1 Introduction

The glaciers of the Canadian Arctic Archipelago have recently experienced a sharp increase in mass wastage in response to anomalously high summer temperatures (Gardner et al., 2011). Between 2006 and 2009 the glaciers of this region lost ice at a rate of $92 \pm 12 \text{ Gt a}^{-1}$, making it the largest contributor to eustatic sea level rise outside of the ice sheets. Of the roughly $146\,000 \text{ km}^2$ of ice in the Canadian Arctic Archipelago, $40\,900 \text{ km}^2$ is located on the southern islands of Baffin and Bylot (Fig. 1). Between 2003 and 2009 these glaciers lost ice at an area-averaged rate 1.6 times greater than the glaciers to the north and twice the rate previously estimated by Abdalati et al. (2004) for the period 1995–2000. Apart from the two short periods of 1995–2000 and 2003–2009, little is known about changes in glacier mass for this region.

Here we focus on glaciers of Baffin and Bylot Islands in order to construct a more complete picture of the spatial patterns of glacier change, and to determine the region's long-term (~50 years) contribution to sea level rise, thereby placing recently observed mass loss rates into a historical context. In previous works (Gardner and Sharp, 2009; Gardner et al., 2011) a surface mass budget model has been used to simulate the long-term glacier mass changes for the northern Canadian

Arctic Archipelago. Applying the same model to simulate long-term glacier changes of Baffin and Bylot Islands was not possible due to a paucity of on-glacier climate observations. We instead construct long-term glacier mass change from changes in elevation that are determined from historical aerial photogrammetry, modern satellite stereoscopic imagery and repeat airborne and satellite laser altimetry. For completeness, we provide an update to the 2003–2009 estimates of Gardner et al. (2011) of glacier mass change derived from repeat satellite gravimetry (GRACE) by including the years 2010 and 2011.

Through our data integration efforts, we are able to assess the extent to which sparse elevation change measurements, in particular those determined from satellite and airborne laser altimetry, can be used to characterize regional-scale glacier change. In addition, multi-temporal estimates of mass change in combination with long-term meteorological records allow us to identify the primary climatic drivers of glacier mass change for this region.

2 Study region

Baffin Island is located to the north of Quebec and Labrador in the territory of Nunavut, Canada (Fig. 1). It covers an area of about 500 000 km², making it the largest island in the Canadian Arctic Archipelago and one of the five largest islands in the world (Andrews et al., 2002). To the northeast lies the heavily glaciated and uninhabited Bylot Island. The glaciers of the two islands cover a total area of 40 900 km² (year ~2000: Fig. 1). The mountainous eastern coast of the region is clustered with icefields and small ice caps (23 600 km² on Baffin and 4900 km² on Bylot) within a ~100 km distance from the ocean (Fig. 1). Extending farther inland on Baffin Island, there are two major ice caps, Barnes and Penny, that cover an area of 5900 km² and 6500 km² respectively. Baffin Island is of particular glaciological importance as it may have played a role in the initiation of the Laurentide Ice Sheet some 116 thousand years ago (Clark et al., 1993), the remnants of which still exist today in the two large ice caps (Hooke, 1976; Fisher et al., 1998; Zdanowicz et al., 2002).

Scientific research on the glaciers of this region first began in the early 1950s and has focused primarily on the two major ice caps (Ward, 1954; Orvig, 1954, 1951; Baird, 1952). Only a handful of in situ conventional and geodetic glacier observations exist for the Barnes Ice Cap (1950 (Ward, 1954), 1962–1966 (Sagar, 1966), 1965–1966 (Løken and Sagar, 1967), 1970–1984 (Hooke et al., 1987) and 1984–2006 (Sneed et al., 2008)), the Penny Ice Cap (1953 (Ward, 1954), 2008–present (Geological Survey of Canada)) and a small valley glacier situated to the northeast of the Penny Ice Cap (1969–1976 (Weaver, 1975)). There are also observations of modern changes in the margin positions of the Barnes Ice Cap (Jacobs et al., 1993, 1997) and some 662

glaciers located on the Cumberland Peninsula, southern Baffin Island (Paul and Svoboda, 2009). For Bylot Island, a comprehensive study of late 1800s, 1958/61 and 2001 valley glacier extents was completed by Dowdeswell et al. (2007). These local studies indicate that the glaciers of Baffin and Bylot Island have been in a state of mass loss and retreat since at least the 1950s.

The first regional estimate of glacier mass change was done by Abdalati et al. (2004) using repeat airborne laser altimetry collected over the Barnes and Penny Ice Caps in spring 1995 and spring 2000. Assuming that the measured elevation change gradients with respect to surface elevation were representative of all glaciers in the region, they estimated that the glaciers of Baffin Island lost ice at an average rate of 10.2 Gt a⁻¹ (assuming an ice density of 900 kg m⁻³). More recently, Gardner et al. (2011) used repeat satellite altimetry (ICESat) and gravimetry (GRACE) to show that the rate of ice loss from the entire region (Baffin + Bylot) had more than doubled to 24 Gt a⁻¹ for the period fall 2003 to fall 2009.

3 Data and methods

3.1 Glacier complex outlines

Outlines of glacier complexes were compiled from 214 individual CanVec maps, a digital cartographic reference product produced by Natural Resources Canada (acquired from: www.GeoGratis.gc.ca). An additional 5500 km² of glacier area not covered by Edition 9 of the CanVec data set were taken from an expanded inventory of Paul and Svoboda (2009). All outlines are based on late-summer Landsat imagery acquired between 1999 and 2004 with the exception of 13 CanVec maps that used late-summer SPOT 5 imagery acquired between 2006 and 2010 and 7 CanVec maps that used 1958 or 1982 aerial photographs. We visually checked the glacier outlines against late-summer Landsat imagery. Some manual editing was done to reclassify a small fraction of ice coverage (<1%) that was missed by the CanVec data set due to incorrect classification over debris cover and supraglacial lakes. The overall quality of the data set was found to be very high.

The new glacier inventory gives a total glacier-covered area of 36 000 km² for Baffin Island and 4900 km² for Bylot Island (Fig. 1). These areas are respectively 2 ± 2% and 4 ± 3% smaller than a range of estimates published in the 1950s and 1960s (see Table 2 in Ommanney, 1971). The smaller area of our data set is attributed to both long-term glacier retreat and methodological differences in glacier delineation.

3.2 Elevation data sets

To determine changes in glacier elevations through time, we difference a number of elevation products. We use Canadian

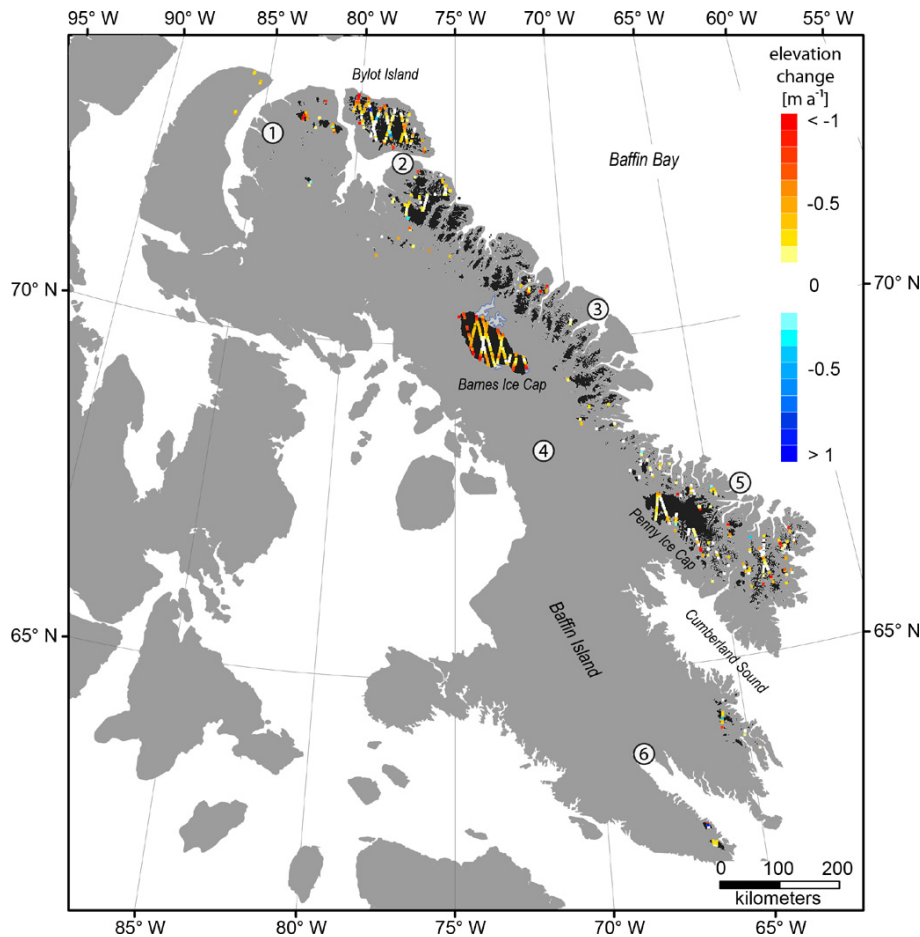


Fig. 1. Elevation change (m a^{-1}) between 1962 and 2006 as determined from ICESat satellite laser altimetry and DEMs generated from airborne stereoscopic imagery (CDED). Numbered dots show the locations of the Environment Canada weather stations used to characterize regional climate (Nanisivik (1), Pond Inlet (2), Clyde River (3), Dewar Lakes (4), Fox Five (5) and Iqaluit (6)).

Digital Elevation Data (CDED) for historical (1952–1983) elevations, and for modern elevations we use SPOT 5 HRS digital elevation models (DEMs: 2008–2010), ICESat satellite laser altimetry (2003–2009), and NASA IceBridge Airborne Topographic Mapper laser altimetry (1995–2011). The data sets have varying temporal and spatial coverage and are generated using different methods.

3.2.1 Historic Canadian Digital Elevation Data (CDED)

Canadian Digital Elevation Data (CDED) were provided at a scale of 1:50k. Horizontal coordinates are in North American Datum 1983 (NAD83), and elevations are orthometric with respect to the mean sea level of the Canadian Vertical Geodetic Datum of 1928 (CVGD28). The data set has a horizontal resolution of 23 m in the north–south direction and 8–17 m in the east–west direction. We used Edition 3.0 of the CDED 1 : 50k data set that was created primarily from historical aerial photographs by stereo-compilation using control points from the Canadian Aerial Survey Database. Maps over

areas with incomplete air photo coverage or insufficient image contrast (primarily over ice and snow) were created from modern DEMs generated from satellite stereoscopic imagery (SPOT 5) and radar interferometry (ERS). All CDED containing modern elevations are excluded from our study. A previous validation of 21 high Arctic CDED maps against ICESat laser altimetry showed the data set to be of high accuracy with a mean offset of +0.3 m above ICESat postings and a standard deviation of 6.2 m (Beaulieu and Clavet, 2009). We performed a similar assessment of the 340 CDED maps used in this study against plane-filtered ICESat data (see Sect. 3.2.3). The CDED had a mean offset of +1.1 m above ICESat postings, a standard deviation of 5.1 m, and very good horizontal control. The exception to this was map sheet 026p03 that covers the south-west margin of the Penny Ice Cap, which we removed from the analysis because of large negative elevation biases relative to ICESat.

At the time of writing, the CDED 1 : 50k data set was still a work in progress and had incomplete coverage for the Canadian Arctic. Complete CDED coverage was only available at

a scale of 1:250k and was created from the digitization of National Topographic System (NTS) maps; however, we found the quality of this data set (-3.2 ± 20.7 m) to be insufficient for elevation change measurement.

3.2.2 SPOT 5 digital elevation models (DEMs)

SPOT 5 HRS (High Resolution Stereoscopic) DEMs were provided by the French Space Agency (CNES) through the SPIRIT International Polar Year project (Korona et al., 2009). The DEMs come in two versions with respective reliability masks that were generated with sets of correlation parameters adapted to different types of relief: Version 1 is optimized for gentle terrain, and Version 2 is optimized for rugged terrain. The DEMs have a horizontal resolution of 40 m, a maximum ground coverage of 120 km by 600 km, and orthometric elevations referenced to the EGM96 geoid. The DEMs were extracted using a 100% automatic processing method that included no manual intervention and no interactive check against any kind of ground-based measurements (Korona et al., 2009). The reliability masks provide grid cell correlation scores of the DEM generation and identify interpolated pixels. Similar DEMs produced for other regions have been found to be highly suitable for elevation change detection over complex glaciated terrain after applying proper bias corrections (Gardelle et al., 2012a; Berthier et al., 2010).

One pair of SPOT DEMs were acquired over Bylot Island (10 January 2008), one pair over the northeastern tip of Baffin Island (19 July 2010), two pairs (A & B) over the Barnes Ice Cap (3 October 2008, 31 August 2010), one pair over the Penny Ice Cap (7 July 2010), and one pair over the Cumberland Peninsula (directly south of the Penny Ice Cap, 3 October 2010). SPOT elevations were first referenced to the WGS84 ellipsoid, and all interpolated pixels (reliability masks of 0 or >100) were excluded. The accuracy of non-interpolated pixels was then assessed using plane-filtered ICESat elevations (Sect. 3.2.3) acquired within ± 90 days of the SPOT acquisition date for ice-covered terrain and all June to October (minimal snow cover) elevations for ice-free terrain. For those DEMs generated from 2010 imagery (Table A1), elevations over ice were taken from the prior year since ICESat was not operational in 2010. From this analysis an optimal reliability masks threshold was individually selected for each of the SPOT DEMs (Fig. A1). Comparisons of valid SPOT elevations against CDED and ICESat altimetry reveal that the SPOT DEMs contain horizontal positioning errors between 7 m and 29 m (Table A2) and elevation biases ranging from -13 m to $+5$ m (Table A1). Despite the large absolute errors, the relative accuracy of the SPOT DEMs is very good with standard deviations in the range 2–5 m over ice-free ground and 1–14 m over glacier surfaces with respect to near-coincident ICESat altimetry (Table A1). There is very little difference between DEM versions except for the Barnes_A DEMs, where Version 1 has better cov-

erage and a lower standard deviation over glacier surfaces than Version 2. The SPOT imagery acquired in late August of 2010 (Barnes_B) had much better contrast than the October 2008 imagery (Barnes_A), resulting in fewer interpolated pixels (better coverage) in the Barnes_B DEM. Therefore, the Barnes_A DEM was only used to estimate elevation change for areas not covered by the Barnes_B DEM. There is very little historic (pre-1983) CDED coverage for the north Baffin SPOT DEMs, so we chose to not include them in our glacier elevation change analysis.

3.2.3 Satellite laser altimetry (ICESat)

The Geoscience Laser Altimeter System (GLAS) onboard ICESat (Zwally et al., 2002) collected surface elevation profiles over 17 repeated observation campaigns between October 2003 and October 2009. GLAS determines surface elevations from laser pulse footprints that have a diameter of ~ 70 m at a spacing of ~ 170 m along each track. We used elevation postings from Release 531 of the GLA06 altimetry product (Zwally et al., 2011b). We converted the data to the WGS84 datum and applied a saturation range correction that is provided with the product. In order to remove potential outlier data from cloud-affected returns, we examined elevation deviations from planes that were fitted 700 m long segments of near repeat-track data (Smith et al., 2009; Moholdt et al., 2010). Elevations that deviated more than 5 m from the calculated plane were excluded from the analysis. In this approach we assume a constant change in elevation with time for each plane when estimated over ice and no change in elevation with time when estimated over ground. Planes were only calculated if they contained a minimum of 4 repeat-track profiles and 10 elevation points. This filtering approach removes about one-third of the data, but ensures a data set free of gross errors.

The uncertainty of the filtered ICESat elevations is estimated to be 0.89 m based on the root-mean-square (RMS) difference at 340 northern and southern Canadian Arctic Archipelago crossover points between ascending and descending tracks within individual observation campaigns (<35 days). Similarly, the standard error of elevation change rates (dh/dt) determined for planes is 0.36 m a^{-1} based on 296 crossovers. These errors can be due to unresolved surface slopes, temporal variations in rates of elevation change, atmospheric forward scattering, detector saturation, off-nadir pointing and errors in satellite range and positioning (e.g. Siegfried et al., 2011; Fricker et al., 2005; Schutz et al., 2005). Correlated errors (bias) are likely smaller than 0.1 m for individual measurement campaigns and 0.01 m a^{-1} for the derived elevation change rates (Zwally et al., 2011a).

3.2.4 Airborne laser altimetry (ATM)

Repeat track airborne laser altimetry was conducted over the Barnes and Penny Ice Caps using the NASA IceBridge

Airborne Topographic Mapper (ATM) in May and June of 1995, 2000, 2005 and 2011 (Barnes Ice Cap only). The ATM system uses a conical scanning laser to measure surface elevations, the footprint and shot spacing of which have changed over time as the ATM hardware has evolved. The system used for the 1995, 2000 and 2005 data has a ~ 140 m swath, with each laser shot having a 1–3 m footprint, a ground spacing of 2–5 m, and a nominal accuracy of <0.2 m (Krabill et al., 2002; Abdalati et al., 2004). The 2011 data were collected with a newer system that has a ~ 230 m swath, a measurement density of ~ 1 per 10 m^2 , a laser footprint of ~ 0.5 m and a nominal accuracy of <0.1 m. Because the majority of transects in our study area were flown over relatively featureless ice caps, we used the Icessn product that is a resampled version of the raw laser data (Krabill, 2011). For the Icessn product, a block of points is selected at ~ 0.5 s smoothing interval, which is ~ 50 m distance along track (actual distance depends on the aircraft speed). The output interval is half the smoothing interval, producing a 50 % overlap between successive platelets. For each smoothing interval, there are three platelets produced in the across-track direction, as well as an 80 m platelet located at aircraft nadir. We used all 4 platelets in our elevation change comparisons.

3.3 Elevation change

Long-term (29–50 years) changes in glacier elevation were determined by differencing historical CDED with recent SPOT DEMs and ICESat altimetry. For the Barnes Ice Cap, we also differenced historical CDED with ATM altimetry. Short-term (5–16 years) elevation changes were determined through differencing of repeat-track laser altimetry from ATM and ICESat.

3.3.1 SPOT versus CDED

Between 40 and 120 individual 1 : 50k CDED map sheets were mosaiced together to cover each of the 5 pairs of SPOT DEMs. The CDED mosaics were first projected and resampled to the SPOT DEM grid in the UTM map projection of the WGS84 datum. All CDED elevations acquired after 1983 were excluded. The SPOT and mosaiced CDED were then co-registered over ice-free surfaces following an iterative process that corrects for the horizontal and vertical offsets using a simple trigonometric relation between aspect, slope and offset (Nuth and Kääb, 2011). To ensure that there is no cumulative degradation of the elevation data, elevations were resampled from their original sources at each iteration of the co-registration process.

The relative accuracy of the DEMs were investigated by differencing the co-registered DEMs from each other over ice-free ground (Table A2). Large elevation differences (dh) were sometimes observed near the modern glacier margins where the ice has retreated over the study period. To make sure that these anomalous values were not included in our

examination of ice-free dh , we only included ice-free areas outside of a 1 km buffer surrounding the glaciers. The dh values were then checked for correlated spatial-, slope-, elevation-, and maximum curvature-dependent biases over ice-free ground (Fig. A2). Of these three biases, only spatially and maximum curvature correlated biases were detected and corrected for. Spatially dependent biases can result from spatially varying phenomena such as air photo coverage, glacial isostatic adjustment, errors in ground control points and errors in geoid transformations. Maximum curvature-dependent biases are associated with differences in horizontal resolution between elevation products (Gardelle et al., 2012b).

After applying bias corrections to the DEMs, we differenced them over glacier surfaces to determine elevation changes (dh) between the CDED and SPOT image acquisition dates. The merged CDED over Bylot Island and the Penny Ice Cap were found to have poor elevation control at higher elevations relative to the SPOT DEMs and ICESat. We removed these errors by applying an iterative standard deviation filter to dh/dt values above 400 m that excludes all values exceeding one standard deviation from the median within 100 m elevation intervals until the standard deviation of each interval is less than 0.3 m a^{-1} . This filter reduced the coverage over ice by about 25 % over Bylot Island and 1–8 % elsewhere. Overall the filter has little impact on the area-averaged elevation change ($<0.02\text{ m a}^{-1}$) indicating that errors in the CDED and/or SPOT DEM are likely not biased. The workflow of the SPOT versus CDED co-registration and differencing is provided in Appendix A (Fig. A2).

3.3.2 CDED versus ICESat

The ICESat-CDED differencing follows a similar approach as the SPOT-CDED differencing (Sect. 3.3.1) except that CDED elevations were extracted at ICESat postings by means of bilinear interpolation and we did not apply an iterative standard deviation filter. No significant horizontal misalignment was detected between CDED and ICESat, so the CDED DEMs were only adjusted vertically for a small mean bias (-1.1 m) and spatially correlated biases as determined over ice-free ground (Table A2). Over the Penny Ice Cap, we have excluded reference track number 18 that indicates unrealistically high rates of thinning at high elevations. A detailed description of the CDED versus ICESat workflow (Fig. A3) and map showing the location of the ICESat elevation used for the ICESat-CDED differencing (Fig. A4) are provided in Appendix A.

3.3.3 Repeat ATM

Elevation changes for the periods 1995–2000, 2000–2005 and 2005–2011 were calculated from repeat ATM airborne laser altimetry by searching for the closest pairs of platelet centroids from two different campaign years, using a search

radius of 100 m (Krabill et al., 2000). We then interpolated the average plateau elevation to the midpoint between the two centroids, based on the reported plateau slopes. Application of this approach to estimate elevation changes of the Greenland Ice Sheet was found to have an elevation change error of 0.085 m (Krabill et al., 2002). When averaged over tens of kilometers, this error reduced to 0.07 m. We manually removed a small subset of the 1995–2000 elevation changes that were obvious outliers (elevation changes >200 m).

In 2011 an extensive flight grid was flown over the Barnes Ice Cap that had sufficient sampling of ice-free terrain to allow for vertical co-registration and differencing with historic CDED. Following the same methodology as outlined for the ICESat-CDED differencing, we were able to determine 1960–2011 mass changes over the Barnes Ice Cap. We then subtracted the repeat ATM estimates of mass change for the period 1995–2011 to determine the 1960–1995 mass change, hence providing a better time chronology of mass changes for the Barnes Ice Cap.

3.3.4 Repeat ICESat

Glacier elevation change rates (dh/dt) were calculated from the plane fitting technique as described in Sect. 3.2.3. Due to filtering and data loss from clouds, all planes do not span the entire ICESat repeat-track period from October 2003 to October 2009. We set a minimum time span requirement of 2 years for each dh/dt . Additionally, we filtered the start and end campaigns of each plane such that they always span an integer number of years; i.e. our ICESat dh/dt estimates are not affected by seasonal biases from accumulation/ablation (Moholdt et al., 2010).

3.4 Mass change

3.4.1 From elevation changes

Volume changes (dV/dt) were estimated for each elevation change data set by first calculating the mean elevation change rate (dh/dt) within each 50 m elevation interval, after applying a 3 sigma filter within each interval to reduce signal noise. Our estimates are insensitive to the use of elevation interval means versus medians for determination of dV/dt ; all estimates agree within $\pm 0.04 \text{ m a}^{-1}$. Unsampled intervals were linearly interpolated from neighboring values. Intervals above and below the sampled elevation range were set to the median value of the first and last three sampled intervals, respectively. dV/dt was then estimated by multiplying the mean dh/dt of each elevation interval by the corresponding surface areas within the intervals as determined from the 1 : 250k CDED. The choice of DEM used for the hypsometrical extrapolation of dh/dt has shown to have little impact on regional volume change estimates (Gardner et al., 2011, supplementary information). The temporal interval of dV/dt is determined from the mean date of all valid CDED, SPOT,

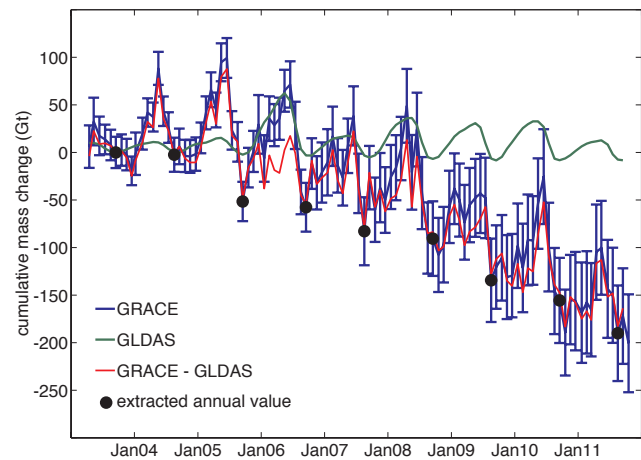


Fig. 2. Baffin and Bylot Island monthly cumulative mass change from GRACE shown in blue (with 95 % confidence intervals), from GLDAS shown in green, and for GRACE corrected with GLDAS shown in red. Black dots show summer minima selected as annual markers.

ICESat and/or ATM elevations. dV/dt was then converted into mass change rates (dM/dt) by applying a constant glacier density of 900 kg m^{-3} .

3.4.2 From GRACE gravimetry

We provide an update to the Gardner et al. (2011) southern Canadian Archipelago (Baffin and Bylot Islands) glacier mass changes derived from repeat gravity observations collected by the GRACE mission. The GRACE satellites measure the temporal variations of the Earth's geopotential field at a monthly interval, distributed as spherical harmonic coefficients up to degree and order 60, from which the redistribution of surface mass can be retrieved (Wahr et al., 1998). The spatial resolution of these fields is limited to a few hundred kilometers, and the data need to be post-processed and filtered to reduce noise in the observations (see Wouters and Schrama, 2007, and Gardner et al., 2011, for a detailed discussion of the processing). This implies that the GRACE satellites do not make point-observations, but that an observation at a certain location is representative for a larger area. As a result, glacier mass loss cannot be directly obtained by taking a simple area integral over the glacier surfaces. The absence of short wavelength information, in combination with the filtering, will bias the signal within the target area. Additionally, signals from adjacent locations, such as hydrology and glacial isostatic adjustment (GIA), when not properly corrected for, may “leak into” the target area and affect the average (see e.g. Swenson and Wahr, 2002). To counter these problems, we use the iterative method of Wouters et al. (2008): In brief, Baffin and Bylot Islands and the surrounding regions were separated into basins (Fig. S1 of Gardner et al., 2011) to which an initial, random mass anomaly is prescribed (we have verified that final result of

the iteration does not depend on the initial values). By applying the same processing steps to these fields as to the real GRACE (CSR RL04) data, pseudo-observations were created and compared to the actual GRACE observations. In an iterative process, the mass anomalies in the basins were adjusted until an optimal agreement in a least-square sense is reached with the GRACE observations.

To isolate the glacier signal, gravity changes associated with GIA were removed using a modified version of the ICE5-G (VM2) model (Peltier, 2004), as described in Riva et al. (2009). No significant gravity trends due to ice loading and unloading during the Little Ice Age are expected in the region (Jacob et al., 2012). Atmospheric mass variations from European Centre for Medium-Range Weather Forecasts (ECMWF) operational pressure fields are removed by the GRACE science teams during processing of the raw satellite data. Likewise, a baroclinic ocean model in combination with a tide model is used to account for mass variations in the ocean (Bettadpur, 2007). To further reduce ocean effects, we estimated mass anomalies in adjacent ocean basins during the iterative procedure, simultaneously with the glacier and terrestrial water storage variations. Due to the small size of the target area, the signal-to-noise ratio in the time series is relatively high. As is evident from Fig. 2, interannual changes and trends are very well captured by the GRACE satellites, but the interpretation of month-to-month variations is less straightforward. Therefore, we select the annual value to be the most negative mass value observed at the end of each ablation season (August to September).

3.5 Uncertainty analysis

3.5.1 Mass changes from elevation changes

Sources of uncertainty in our mass change estimates are primarily from uncertainties in the following: the measurement of dh , dh due to glacial isostatic adjustment, changes in glacier area through time, extrapolation of dh to determine regional dV , mean glacier density, and trends in firn density from changes in precipitation, compaction rates and internal accumulation. All uncertainties are given as 95 % confidence intervals. To characterize the measurement uncertainties for long-term differencing that are co-registered over ice-free terrain, we examined semivariograms of the elevation difference over non-ice surfaces. After adjusting for identifiable biases, there were still large-scale correlations evident in the SPOT-CDED semivariograms, and a more clearly defined correlation length of 50 km in the ICESat-CDED semivariogram (cf. Rolstad et al., 2009). The approximate diagonal length of the largest CDED map used in the study is 50 km, indicating that dh errors are likely correlated by individual CDED map coverage. Therefore, we applied standard error propagation at a correlation length of 50 km to the standard deviation between elevation products over ice-free terrain to estimate the measurement uncertainty for the ICESat-CDED,

SPOT-CDED, and ATM-CDED differencing (multiplied by 1.96 to get the 95 % confidence intervals). For ATM-ATM differencing we assigned a correlated repeat measurement uncertainty of 0.14 m ($\sim 1.96 \times 0.07$ m standard error) as estimated by Krabill et al. (2002), and for the ICESat-ICESat differencing we assigned an uncertainty of 0.69 m a^{-1} with an along-track correlation length of 5 km (Moholdt et al., 2010). To account for small biases resulting from glacial isostatic adjustment, we added a correlated uncertainty of 6 mm a^{-1} to all repeat altimetry elevation change estimates (Gardner et al., 2011). This was not necessary for the ICESat-CDED, SPOT-CDED, or ATM-CDED differencing, as elevation products were co-registered over ice-free terrain.

To account for changes in glacier area through time, we assigned an uncertainty of $\pm 10\%$ to all dV/dt estimates. To test if the assigned uncertainty interval of $\pm 10\%$ is appropriate, we re-ran our analysis with 1.5 % more ice added evenly to the lowest 400 m of the glacier hypsometry within each region. We chose 1.5 % as this is roughly the midpoint between area differences (see Sect. 3.1) and can be expected to be the net effect on time-averaged mass change estimates. Changing the glacier hypsometry in this way resulted in sub-region losses that were $4 \pm 3\%$ larger than the unperturbed estimate. Since changes in area are not well constrained, we retain an uncertainty of $\pm 10\%$. The ICESat and ATM differencing have additional uncertainties in dV/dt due to the extrapolation of dh/dt elevation profiles across each region. For the ICESat-CDED and ATM-ATM differencing, this was characterized by using subsets of the 2004–2009 ICESat elevation change rates (dh/dt) as analogs for the spatial sampling of dh/dt for the ICESat-CDED and ATM data sets. The dh/dt subsets were selected from a 5 km buffer zone around the ICESat-CDED and ATM postings, respectively (Fig. A4). The 95 % confidence interval for the extrapolation from dh/dt to dV/dt was taken to be 1.96 times the percentage difference in dV/dt between using all 2004–2009 ICESat data and a subset. Using this approach we determined uncertainties of 4 % and 31 % for the extrapolation of ATM dh/dt profiles over the Barnes and Penny Ice Caps, respectively. Using ATM dh/dt profiles over the Penny Ice Cap to determine the volume change of the remaining glaciers on Baffin and Bylot Islands introduced an uncertainty of 61 %, which is lower than if data from the Barnes Ice Cap are used. In all cases, extrapolation of the ATM data resulted in an apparent overestimation of mass loss, which indicates that the two ice caps are ablating more rapidly than the coastal icefields. CDED are not complete over the accumulation area of the Penny Ice Cap (Fig. 1), so extrapolation of ICESat-CDED results over the entire ice cap introduced an uncertainty of 24 %. Similarly, extrapolation of ICESat-CDED results outside of Bylot Island and the two ice caps introduced volume change uncertainties of 6 % and 12 % for the remaining glacier ice to the south and north of 68.6° N , respectively. Volume change uncertainties from the extrapolation of SPOT-CDED results over Bylot Island, the Penny

Ice Cap, and the southern glaciers, extrapolation of ICESat-CDED results over Bylot Island and the Barnes Ice Cap, and the extrapolation of ICESat-ICESat results over all regions could not be estimated in the same way as done for the ICESat-CDED and ATM-ATM results. These estimates were assigned an uncertainty of 10 %.

To convert from dV/dt to dM/dt , we applied a constant glacier density of 900 kg m^{-3} , to which we assigned an assumed uncertainty of $\pm 17 \text{ kg m}^{-3}$. This approach assumes a constant firn density over the past 50 years (i.e. Sorge's law applies (Bader, 1954)). This is likely not a valid assumption as rapid changes in glacier mass have recently been observed (Gardner et al., 2011; Fisher et al., 2012). Zdanowicz et al. (2012) found that there was almost no change in the near-surface (upper 20 m) vertical density-profile between ice cores from 1979 and 1995 collected at elevations of 1975 m and 1860 m on the Penny Ice Cap (Holdsworth, 1984; Fisher et al., 1998). However, comparison with a 2010 core collected at the same location shows that the depth-averaged 20 m density has increased by about 34 kg m^{-3} ($2.2 \text{ kg m}^{-3} \text{ a}^{-1}$) since 1995 and is nearly identical to the mean density of a 1953 shallow ice core collected 30 km to the south-southeast at an elevation of 1930 m (Ward, 1954). This suggests that the assumption of a constant density profile is likely appropriate for the multi-decadal elevation differences but may introduce errors in shorter-term studies. For example, if the average density of the top 20 m of all glacier areas above the equilibrium line altitude ($\sim 1400 \text{ m}$) increased at a rate of $2.2 \text{ kg m}^{-3} \text{ a}^{-1}$, the application of Sorge's law would result in a 0.23 Gt a^{-1} overestimate of glacier mass loss from the region. Unfortunately, the regional changes in firn density are not well enough constrained to justify modifying our mass change estimates. We instead assigned an uncertainty of $4 \text{ kg m}^{-3} \text{ a}^{-1}$ to areas above 1400 m to account for changes in the 20 m density profile for studies spanning less than 20 years (repeat ATM and ICESat) and $2 \text{ kg m}^{-3} \text{ a}^{-1}$ for studies spanning 20 years or more (comparisons with CDED). Note that this uncertainty comes in addition to the uncertainty in mean density ($\pm 17 \text{ kg m}^{-3}$).

To determine the total uncertainty, we assumed that all individual sources are correlated in space but uncorrelated with each other; i.e. the total uncertainty for each region was taken as the root sum of squares (RSS) of individual uncertainties. For the total uncertainty of all ice area, we sum each of the separate sources of uncertainty for each region then take the RSS of the summed individual components to determine the total uncertainty. All uncertainties associated with the derivation of mass changes from the various elevation change products are provided in Table 1.

3.5.2 Mass changes from GRACE gravimetry

The GRACE trends in the Arctic region are dominated by the mass change signal of the Greenland Ice Sheet that may affect the retrieval of the mass variations over Baffin and By-

lot Islands. Simulations with pseudo-observations based on a combination of models, representative for mass variations in the cryosphere, terrestrial water storage and ocean, have shown that the trends in glacier mass for Baffin and Bylot Islands can be retrieved to within $\pm 3 \text{ Gt a}^{-1}$ (Gardner et al., 2011), indicating that our Baffin and Bylot Islands estimates are not significantly affected by the mass loss of the Greenland Ice Sheet.

The geopotential anomalies observed by the GRACE satellites are the sum of mass variations in various components of the Earth system that need to be removed before the glacier mass anomalies can be estimated. Uncertainties in these corrections are included in the overall error bars. We assessed the uncertainty of the atmospheric correction by comparing ECMWF and National Centers for Environmental Prediction Reanalysis (NCEP R1). The trend in atmospheric loading over Baffin and Bylot Islands shows no significant differences between these two products ($0.1 \pm 0.1 \text{ Gt a}^{-1}$). Uncertainty in the GIA correction that results from incomplete knowledge of the Earth's structure and ice loading history is estimated to be 4.9 Gt a^{-1} for Baffin and Bylot Islands. This uncertainty was determined by considering a range of realistic viscosity profiles of 0.3×10^{21} to $1 \times 10^{21} \text{ Pa s}$ and 0.3×10^{21} to $1 \times 10^{22} \text{ Pa s}$ for the upper and lower mantle, respectively and alternative loading histories [the ICE-3G (Tushingham and Peltier, 1991) and ANU (Lambeck et al., 2004) models]. Note that Gardner et al. (2011) erroneously reported a range for the lower mantle viscosity of 0.3×10^{21} to 3.6×10^{21} ; this should have been the same as reported here.

Due to the coarse spatial resolution of the GRACE data, the basins used in the iterative basin method do not exactly follow the glacier boundaries and partly cover non-glaciated areas. This means that our results do not only track the glaciers' mass budget, but also changes in terrestrial water storage, since GRACE cannot distinguish between the two. The Global Land Data Assimilation System (GLDAS; Rodell et al., 2004) in its NOAA $0.25^\circ \times 0.25^\circ$ configuration gives a very small trend in terrestrial water storage ($< 0.9 \pm 1.2 \text{ Gt a}^{-1}$) when considering the end-of-melt-season dates that were used to estimate annual mass changes from GRACE (August–September; see Fig. 2 and Sect. 3.4.2). The trend in terrestrial water storage is insignificant, so we simply added this to our estimate of uncertainty. In addition to the uncertainties from the GIA and terrestrial water storage, our monthly GRACE solution (Fig. 2) includes measurement error based on sub-set and inter-month comparisons as provided by the GRACE science team. The monthly values differ slightly from those reported in Gardner et al. (2011; see their supplementary Fig. 3). This is a result of post-processing of the GRACE data, which relies on EOF analysis and therefore evolves with the period of observation. Differences are well within the error bars of the monthly GRACE solutions (Fig. 2).

Table 1. Glacier mass change determined from CDED, SPOT, ICESat and ATM elevation data sets with respective uncertainties.

Method	Region	Area [km ²]	Start date	End date	dM/dt		Sources of error (95 % confidence interval) [kg m ⁻² a ⁻¹]						
					[kg m ⁻² a ⁻¹]	[Gt a ⁻¹]	Measurement	GIA	Glacier area [±10 %]	Extrapolation	Bulk density [±17 kg m ⁻³]	Trends in firn density	Total
SPOT-CDED	Barnes	5863	1960	2010	-476	-2.8	85	0	47	0	9	0	97
	Bylot	4875	1979	2008	-277	-1.4	157	0	27	27	5	7	162
	Penny	6508	1958	2009	-166	-1.1	86	0	16	16	3	44	99
	South	7588	1958	2009	-237	-1.8	28	0	23	23	4	6	43
ICESat-CDED	Barnes	5863	1960	2006	-414	-2.4	91	0	41	41	8	0	108
	Bylot	4875	1980	2006	-277	-1.4	162	0	27	27	5	7	167
	Penny	6508	1958	2006	-235	-1.5	80	0	23	55	4	44	109
	North	16065	1963	2006	-263	-4.2	45	0	26	31	5	3	60
	South	7588	1957	2006	-202	-1.5	48	0	20	12	4	6	54
	All	40 899	1962	2006	-271	-11.1	72	0	27	32	5	10	84
ATM-CDED	Barnes	5863	1960	1995	-323	-1.9	114	0	32	13	6	0	119
ATM-ATM	Barnes	5863	1995	2000	-583	-3.4	25	5	57	23	11	0	68
	Penny	6508	1995	2000	-194	-1.3	25	5	19	61	4	87	111
	non ice cap	28528	1995	2000	-369	-10.5	25	5	36	224	7	9	229
	All	40 899	1995	2000	-372	-15.2	25	5	36	169	7	20	176
ATM-ATM	Barnes	5863	2000	2005	-722	-4.2	25	5	71	28	13	0	81
	Penny	6508	2000	2005	-443	-2.9	25	5	43	139	8	87	172
	non ice cap	28528	2000	2005	-647	-18.5	25	5	63	393	12	9	399
	All	40 899	2000	2005	-625	-25.6	25	5	61	300	12	20	308
ATM-ATM	Barnes	5863	2005	2011	-1075	-6.3	21	5	105	42	20	0	117
ICESat-ICESat	Barnes	5863	2003	2009	-844	-5.0	40	5	83	83	16	0	125
	Bylot	4875	2003	2009	-554	-2.7	47	5	54	54	10	15	92
	Penny	6464	2003	2009	-515	-3.3	42	5	50	50	10	88	121
	North	16109	2003	2009	-520	-8.4	33	5	51	51	10	7	80
	South	7588	2003	2009	-759	-5.8	42	5	74	74	14	11	115
	All	40 899	2003	2009	-614	-25.1	39	5	60	60	11	20	96
GRACE	All	40 899	2003	2011	-581	-23.8	86	118	hydrology = 39			149	

3.6 Climate

To help interpret glacier mass changes in terms of regional climate forcing, we examined anomalies in mean summer (JJA) homogenized 2 m air temperatures for 4 Environment Canada weather stations located at Pond Inlet, Clyde River, Dewar Lakes and Iqaluit (Vincent et al., 2002). We also examined anomalies in adjusted total annual precipitation for the 5 weather stations at Pond Inlet, Nanisivik, Dewar Lakes, Fox Five and Iqaluit (Mekis and Vincent, 2011). Temperature and precipitation records discontinuously span the period 1930 to 2010 and 1932 to 2009, respectively. All stations except Dewar Lakes are located near the ocean and are therefore biased towards low-altitude coastal conditions (Fig. 1). For this reason, we also examine summer (June, July, August) glacier area-averaged NCEP R1 “free-air” temperature anomalies at 700 mb geopotential height (Kalnay et al., 1996).

4 Results

4.1 Mass change

Long-term elevation changes determined from the comparison of historic CDED with ICESat laser altimetry and SPOT DEMs are shown in Figs. 1, 3, 4 and 5, and corresponding

mass change estimates are provided in Table 1. The coverage of the Barnes Ice Cap and Bylot Island glaciers is very good for both data sets, but coverage elsewhere is limited by CDED and ICESat availability. Merging results from SPOT Barnes_B V2 and Barnes_A V1 DEMs, we estimated that the Barnes Ice Cap lost mass at a rate of $476 \pm 97 \text{ kg m}^{-2} \text{ a}^{-1}$ between 1960 and 2010. This compares well with a rate of $414 \pm 108 \text{ kg m}^{-2} \text{ a}^{-1}$ as estimated from ICESat for the period 1960 and 2006. Examining the subset of SPOT-CDED dh/dt that is within 1 km of the ICESat tracks indicates that about half of the difference between estimate means can be attributed to differences in spatial sampling. The rest of the difference between the two data sets is likely due to differences in the sampling interval with higher than average losses in the years 2007 through 2010. Despite the ice cap's simple geometry, the map of dh/dt reveals a relatively complex pattern of elevation change (Fig. 3). Thinning rates exceed 1.5 m a^{-1} along the northwestern and southwestern margins and at more localized locations along the northeastern margin where the ice cap abuts proglacial lakes (e.g. Conn and Bieler Lakes). These proglacial lakes have been shown to locally enhance the ice flow of the Barnes Ice Cap (Andrews et al., 2002). Elevation changes are smallest at higher elevations and for one of the southwest lobes that has likely experienced “local creep slump” (i.e. enhanced ice creep and basal sliding; see Holdsworth, 1977, 1973; Andrews et al.,

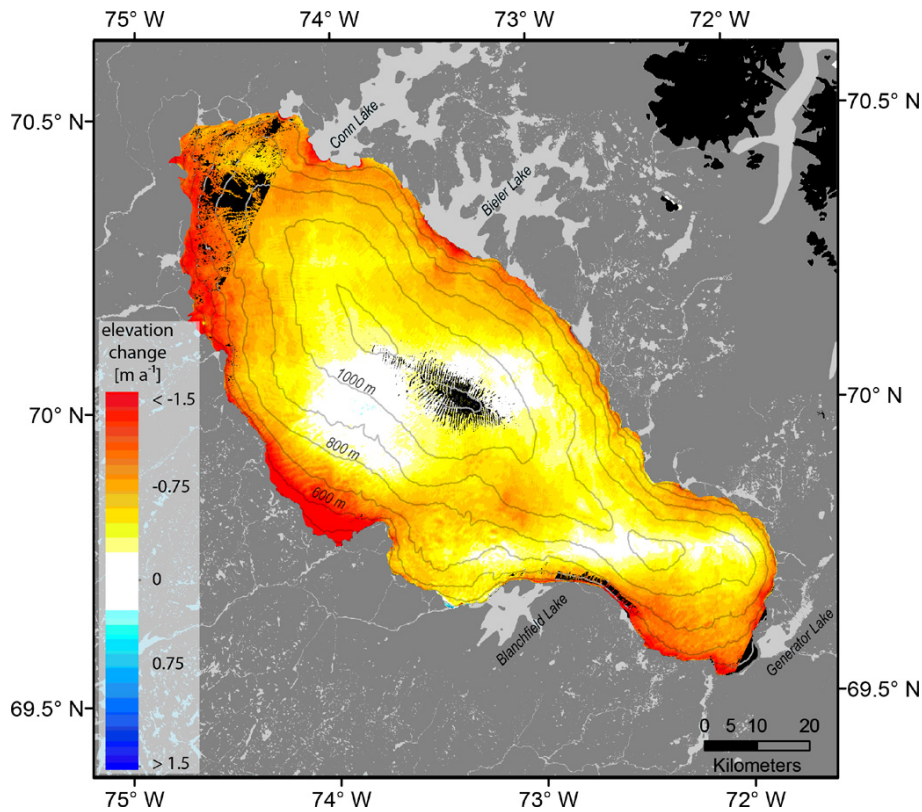


Fig. 3. Elevation change (m a^{-1}) of the Barnes Ice Cap between 1960 and 2010 as determined from DEMs generated from airborne and SPOT-5 satellite stereoscopic imagery. Areas of black indicate no data.

2002), a phenomenon that was also observed by Abdalati et al. (2004) in repeat airborne laser altimetry.

The map of dh/dt for the glaciers of Bylot Island generated from the SPOT Bylot V2 DEM and CDED shows a strong pattern of elevation lowering that is most pronounced at lower elevations (Fig. 4). Most outlet glaciers have experienced an average elevation loss of around $1\text{--}2 \text{ m a}^{-1}$ at their termini. There are, however, four outlet glaciers (B7, C93, D78, and D20) that experienced little terminus elevation change, suggesting that mass input from glacier flow and accumulation has matched surface ablation over this period. This suggests that these glaciers may have experienced part or all of a surge cycle over the sample interval. This inference is in agreement with Dowdeswell et al. (2007) who found that most of the major outlet glaciers on Bylot Island are surge-type. Dowdeswell et al. (2007) also noted that glacier D78, the longest glacier on Bylot Island, had an over-steepened frontal margin and appears to have advanced and overrun its neoglacial terminal moraines. This advance is clearly identified in Fig. 4 as an elevation gain at the terminus of D78.

Overall there is a less coherent spatial pattern of glacier elevation change over Bylot Island than observed over the Barnes Ice Cap. This can be attributed to two factors. First, the CDED covering glacier ice in this region have a mean date of 1979 and the SPOT DEM was generated from 2008

imagery. This means that the dh/dt estimates for Bylot Island cover a period that is 21 years shorter than that derived for the Barnes Ice Cap (i.e. smaller cumulative changes in elevation). Second, the magnitudes of glacier elevation change rates are smaller over Bylot Island than over the ice cap. All of these factors lead to a higher signal-to-noise ratio in the Bylot Island dh/dt estimates. From SPOT-CDED differencing, we estimated that the glaciers of Bylot Island lost ice at a rate of $277 \pm 162 \text{ kg m}^{-2} \text{ a}^{-1}$ over the 29-year period, which is identical to the estimate determined from ICESat-CDED differencing for the period 1980 to 2006.

Outside of Bylot Island and the Barnes Ice Cap, the historic CDED coverage is significantly reduced but still sufficient to determine regionally representative dh/dt elevation profiles and therefore mass changes for the remaining ice. From SPOT-CDED (Fig. 5) and ICESat-CDED (Fig. 1) differencing, we determine mass loss rates of $166 \pm 99 \text{ kg m}^{-2} \text{ a}^{-1}$ (1958–2010) and $235 \pm 109 \text{ kg m}^{-2} \text{ a}^{-1}$ (1958–2006) for the Penny Ice Cap, and $237 \pm 43 \text{ kg m}^{-2} \text{ a}^{-1}$ (1958–2010) and $202 \pm 54 \text{ kg m}^{-2} \text{ a}^{-1}$ (1958–2006) for the 7600 km^2 of glaciers south of 68.6° N excluding the Penny Ice Cap, respectively. From the ICESat-CDED differencing, we determine that the $16\,100 \text{ km}^2$ of glaciers north of 68.6° N , excluding Bylot Island and the Barnes Ice Cap, lost ice at a rate $263 \pm 60 \text{ kg m}^{-2} \text{ a}^{-1}$ (1963–2006). With the

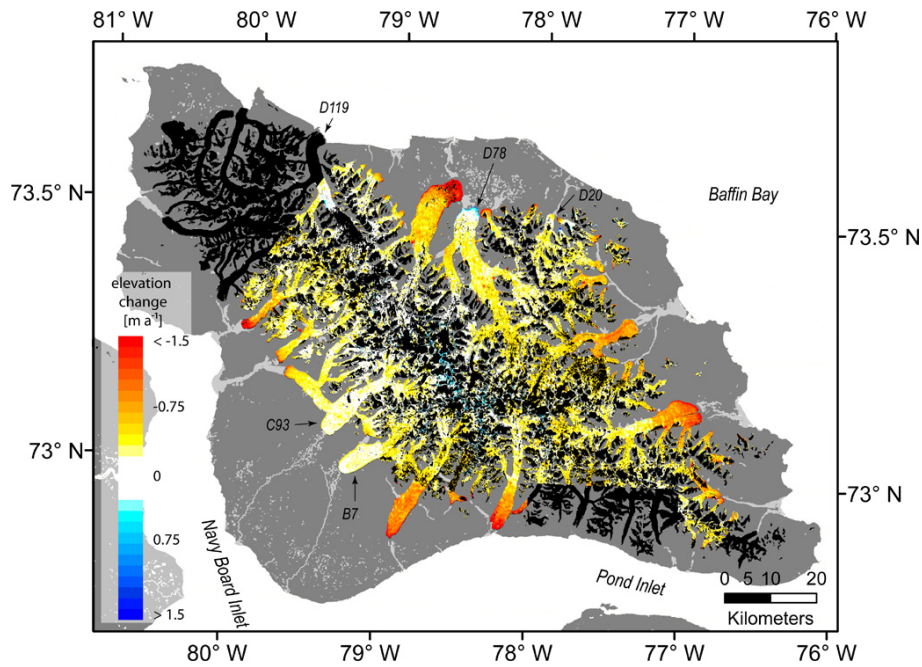


Fig. 4. Elevation change rate (m a^{-1}) of the glaciers of Bylot Island between 1979 and 2008 as determined from DEMs generated from airborne and SPOT-5 satellite stereoscopic imagery. Areas of black indicate no data.

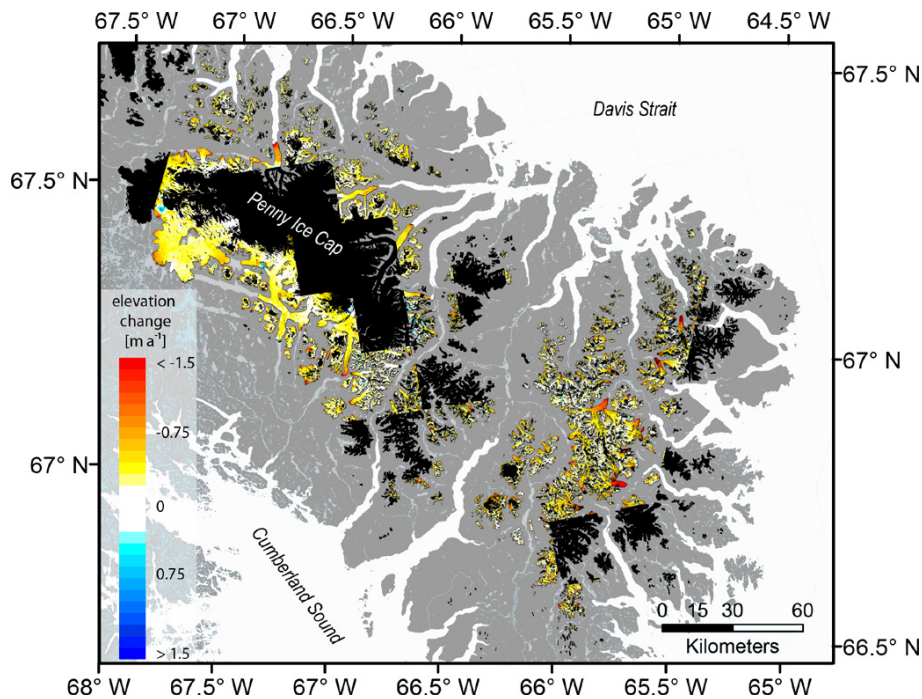


Fig. 5. Elevation change rate (m a^{-1}) of the Penny Ice Cap and the glaciers of the Cumberland Peninsula between 1958 and 2010 as determined from DEMs generated from airborne and SPOT-5 satellite stereoscopic imagery. Areas of black indicate no data.

exception of the Barnes Ice Cap as noted earlier, analysis of the subset of SPOT-CDED data within a 1 km distance of the ICESat tracks indicates no bias due to differences in spatial sampling between the ICESat-CDED and SPOT-

CDED analysis. In total, the glaciers of Baffin and Bylot Islands collectively lost ice at a rate of $271 \pm 84 \text{ kg m}^{-2} \text{ a}^{-1}$ (or $11.1 \text{ Gt a}^{-1} \pm 3.4 \text{ Gt a}^{-1}$) between 1963 and 2006.

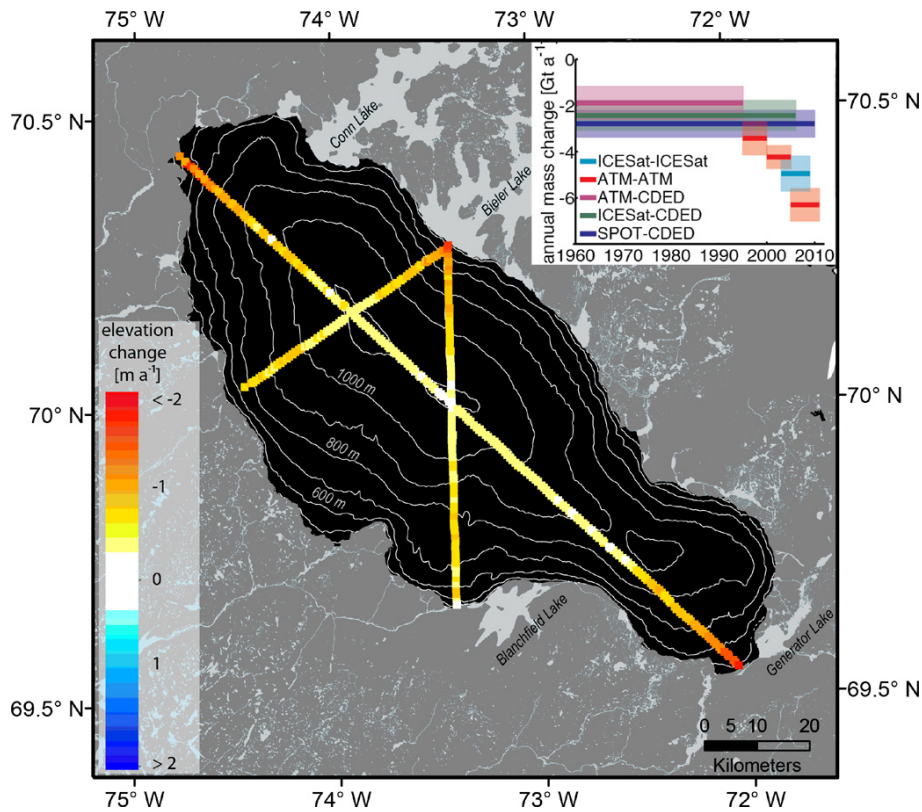


Fig. 6. Elevation change rate (m a^{-1}) of the Barnes Ice Cap between spring 2000 and spring 2005 as determined from repeat airborne laser altimetry. Inset graph shows annual mass change of the Barnes Ice Cap determined over varying time periods with corresponding 95 % confidence intervals. A mass change of $1 \text{ Gt a}^{-1} = 169 \text{ kg m}^{-2} \text{ a}^{-1}$.

The repeat ATM differencing, starting from 1995, shows higher rates of mass loss for the Barnes and Penny Ice Caps than the long-term average. Between spring of 1995 and 2000, the Barnes Ice Cap lost ice at a rate of $583 \pm 68 \text{ kg m}^{-2} \text{ a}^{-1}$, increasing to $722 \pm 81 \text{ kg m}^{-2} \text{ a}^{-1}$ for the period 2000 to 2005 (Fig. 6), and to $1075 \pm 125 \text{ kg m}^{-2} \text{ a}^{-1}$ for the period 2005 to 2011. Similar analysis for the Penny Ice Cap gives mass loss rates of $194 \pm 111 \text{ kg m}^{-2} \text{ a}^{-1}$ for the period 1995 to 2000, increasing to $443 \pm 172 \text{ kg m}^{-2} \text{ a}^{-1}$ for the period 2000 to 2005 (Fig. 7). Unfortunately, there were no ATM flights over the Penny Ice Cap in 2011 due to logistical constraints. Extrapolating elevation changes measured over the Penny Ice Cap to the remaining glacier cover, which performs better than extrapolating Barnes Ice Cap data (see Sect. 3.5.1), gives a total mass loss for the region of $372 \pm 176 \text{ kg m}^{-2} \text{ a}^{-1}$ ($15.2 \pm 7.2 \text{ Gt a}^{-1}$) and $625 \pm 308 \text{ kg m}^{-2} \text{ a}^{-1}$ ($25.6 \pm 12.6 \text{ Gt a}^{-1}$) for the periods 1995–2000 and 2000–2005, respectively. The high uncertainties for the ATM estimates reflect the large area of extrapolation. Comparative extrapolations done with subsets of the 2004–2009 ICESat elevation changes indicate that the ATM estimates are likely biased towards too much loss (see Sect. 3.5.1). That said, we cannot be absolutely certain that the ATM estimates are bi-

ased as the ICESat and ATM data sets do not cover the same time period.

The recent increase in glacier mass loss is confirmed by near repeat-track ICESat laser altimetry. Our results (updated from Gardner et al., 2011, using new glacier hypsometry) indicate a glacier mass loss of $614 \pm 96 \text{ kg m}^{-2} \text{ a}^{-1}$ ($25.1 \pm 4.0 \text{ Gt a}^{-1}$) for Baffin and Bylot Islands between 2003 and 2009, which is not significantly different from the 2000–2005 ATM estimate. The updated GRACE results for Baffin and Bylot Islands also confirm the increased rates of mass loss (Fig. 2). Between 2003 and 2011 GRACE gives an average mass loss of $581 \pm 149 \text{ kg m}^{-2} \text{ a}^{-1}$ ($23.8 \pm 6.1 \text{ Gt a}^{-1}$). Mass change estimates for the region as a whole (Fig. 8) show a clear indication of accelerated melt in recent decades.

4.2 Drivers of increased mass change

The interannual variability of snowfall amounts (accumulation) over the glaciers of Baffin and Bylot Islands is small relative to the interannual variability of ablation, and changes in glacier mass budget are well correlated with changes in summer temperature but not as well with changes in precipitation (Sneed et al., 2008; Hooke et al., 1987; Weaver, 1975). Our analysis of four Environment Canada weather stations shows

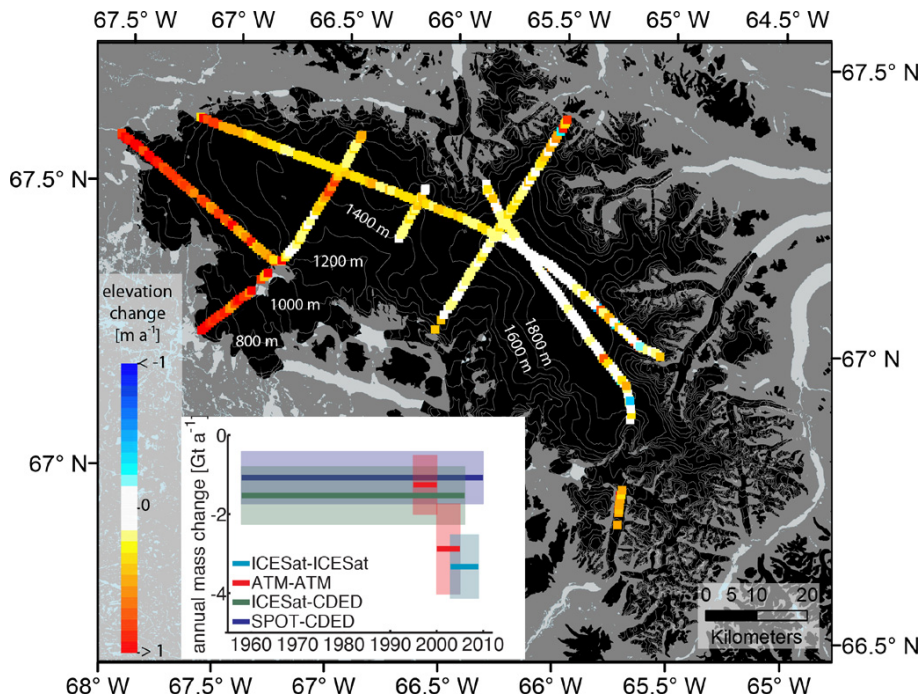


Fig. 7. Elevation change rate (m a^{-1}) of the Penny Ice Cap between spring 2000 and spring 2005 as determined from repeat airborne laser altimetry. Inset graph shows annual mass change of the Penny Ice Cap determined over varying time periods with corresponding 95% confidence intervals. A mass change of $1 \text{ Gt a}^{-1} = 154 \text{ kg m}^{-2} \text{ a}^{-1}$.

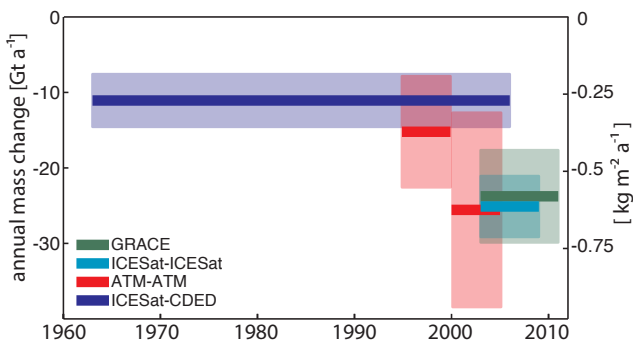


Fig. 8. Mass changes of Baffin and Bylot Island glaciers with corresponding 95 % confidence intervals.

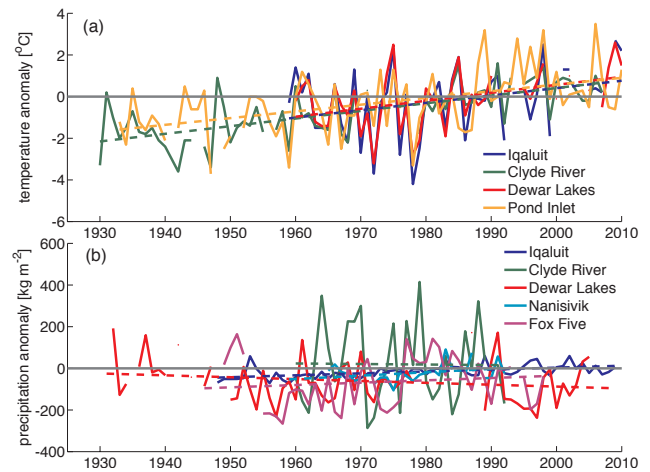


Fig. 9. (a) Summer (June, July, August) temperature and (b) annual precipitation anomalies relative to the 1981–1990 mean (optimal period of overlap). Dashed lines show linear trends fitted to all data from each station.

nearly identical long-term trends in mean summer temperatures of $+0.35 \pm 0.02 \text{ }^{\circ}\text{C}$ per decade (Fig. 9a), and recent analysis of passive microwave data indicates an increase in the number of melt days over the Barnes Ice Cap between 1979–2010 (Dupont et al., 2012). Measuring precipitation amounts in the Arctic is notoriously difficult due to gauge undercatch of solid precipitation and difficulties in correcting gauge biases (Mekis and Hogg, 1999). The sparse measurements that are available indicate that there has been little change in annual precipitation over the period of study (Fig. 9b). This suggests that the increasing mass loss in the region has largely been driven by a long-term increase in

summer temperature. To support this conclusion, we investigated the relationship between mass loss rates and summer glacier area-averaged NCEP R1 700 mb ($\sim 2900 \text{ m a.s.l.}$) temperature anomalies averaged for each mass change interval (Fig. 10a). For the Barnes Ice Cap, there is a nearly perfect linear ($r = -0.99$) relationship between the rate of mass change and summer temperatures of $-405 \text{ kg m}^{-2} \text{ a}^{-1}$ per

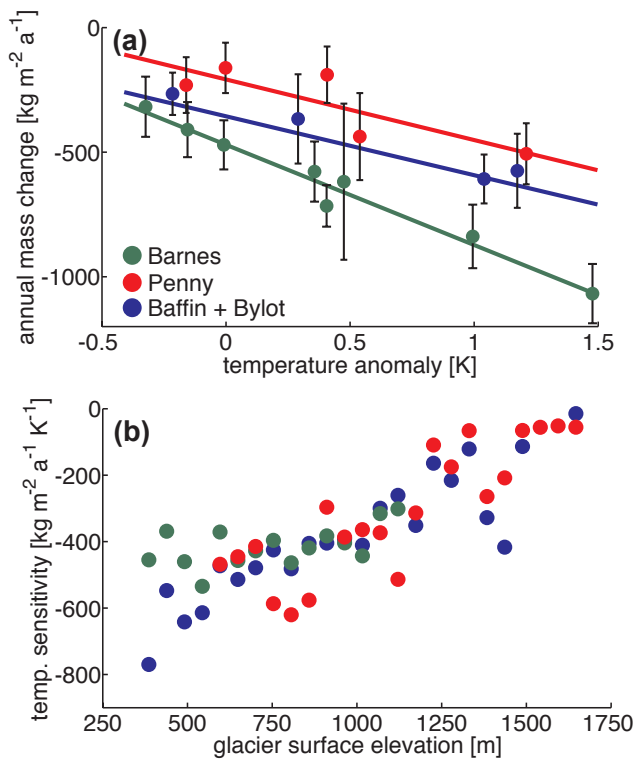


Fig. 10. (a) Glacier area-averaged annual mass change with 95 % confidence intervals plotted against NCEP R1 summer (June, July, August) glacier area-averaged 700 mb temperature anomalies for each mass change measurement interval. Anomalies are relative to the 1960–2010 means. Lines show linear fits with the following slopes: Barnes = -405 ($r = -0.99$), Penny = -245 ($r = -0.84$), and Baffin and Bylot Island glaciers = -238 ($r = -0.84$) with units of $\text{kg m}^{-2} \text{ a}^{-1}$ per 1°C increase in temperature. (b) Annual mass change sensitivity with respect to glacier area-averaged 700 mb summer temperature as a function of glacier surface elevation. (b) shows that glacier surfaces are most sensitive to changes in summer temperature at lower elevation.

1°C . Mass loss rates for the Penny Ice Cap and the region as a whole appear to be less sensitive to changes in summer temperatures (-245 to $-238 \text{ kg m}^{-2} \text{ a}^{-1}$ per 1°C , $r = -0.84$ for both). Looking in more detail, we find that the sensitivity of mass changes to changes in summer temperatures is linearly related to surface elevation (Fig. 10b) and that the relationship between sensitivity and elevation differs little between regions. This elevation dependence explains why the Barnes Ice Cap, which has lower mean elevation than the Penn Ice Cap (Fig. A5), is more sensitive to changes in summer temperature than the Penny Ice Cap.

The link between higher summer temperatures and increased glacier ablation is more complex than may first appear. Higher temperatures lead to more downward longwave radiation and increased sensible heat flux, but these direct links can only account for some of the glacier's sensitivity to temperature. Examining NCEP R1 glacier area-

averaged summer means we find that, for every 1°C increase in 700 mb temperature, there is a corresponding 4.7 W m^{-2} increase in the downward longwave radiative flux at the surface. Over a three-month period, this is enough energy to melt an additional 110 kg m^{-2} of ice at 0°C . Therefore, increased downward longwave radiation directly accounts for less than 27% to 46% of the observed temperature sensitivity. The remaining sensitivity is due to increased sensible heat flux and indirect effects. One of the largest indirect effects is the temperature-albedo feedback that results in higher absorption of downward shortwave radiative flux. Higher temperatures result in enhanced snow grain growth and larger effective grain sizes that reduce the albedo of snow. This increases shortwave absorption, snow temperature and melt, which in-turn can lead to further grain growth (Flanner and Zender, 2006; Gardner and Sharp, 2010). Higher temperatures also result in earlier and more extensive removal of snow. This increases absorption of shortwave radiation by exposing darker glacier ice and firn.

A possible non-climatic driver is the feedback between mass budget and elevation. To assess the possible impact of the elevation feedback on accelerated ice loss, we assume that the dh/dt gradient with elevation is constant over a 50-year period and compare volume change estimates using the original glacier hypsometry and one that is modified to reflect the elevation changes that would have occurred over this time according to the dh/dt gradient. We find that changes in elevation over a 50-year period could account for no more than a $0.03 \text{ kg m}^{-2} \text{ a}^{-1}$ increase in ablation for either ice cap.

5 Comparison with previous studies

Other than Gardner et al. (2011), we are aware of only two other regional estimates of glacier mass change that do not rely on modeling or interpolation of sparse local-scale glaciological measurements. The first is that of Abdalati et al. (2004) who used the ATM data to estimate a mass loss of 10.2 Gt a^{-1} for the Baffin Island glaciers between 1995–2000. This is 3.2 Gt a^{-1} less than our corresponding estimate of 13.4 Gt a^{-1} . We largely attribute these differences to our use of an improved glacier mask (1600 km^2 more ice) that includes more low-lying glacier ice, the characterization of glacier hypsometry using a much higher resolution DEM, and the calculation of dh/dt using the Icessn product that is a resampled version of the raw laser data used by Abdalati et al. The second regional estimate of mass change is from a recent GRACE study (Jacob et al., 2012) that shows higher rate of loss for Baffin and Bylot Island glaciers (2003–2010: $33 \pm 2.5 \text{ Gt a}^{-1}$) than our corresponding GRACE estimate (2003–2009: $23.8 \pm 3.1 \text{ Gt a}^{-1}$) but agree within error bounds. We have reexamined both estimates and it appears that differences in GIA and terrestrial water storage corrections, time interval, and the method used to estimate mass changes (end-of-melt season vs. trend of full time series)

could only account for a small fraction of the difference ($0\text{--}2\text{ Gt a}^{-1}$) between GRACE estimates. Other possible sources for the disagreement are differences in domains, how signals outside the target regions are treated, and the partitioning of mass changes between northern and southern Canadian Arctic regions/mascons. Again, both GRACE estimates agree within error bounds, but a more in-depth examination would still be valuable to identify the source of the disagreement.

It is difficult to compare our regional estimates of glacier mass change with earlier in situ measurements that have small spatial coverage and span short time periods (Ward, 1954; Sagar, 1966; Løken and Sagar, 1967; Weaver, 1975). The only place a reasonable comparison with pre-ATM (1995) estimates can be made is for the Barnes Ice Cap where long-term elevation differences have been measured for a summit-to-terminus transect along the north-east lobe of the ice cap (Hooke et al., 1987; Sneed et al., 2008). Using theodolites, GPS, an ASTER DEM, and ICESat altimetry, and averaging over the length of the transect, Hooke et al. (1987) and Sneed et al. (2008) estimated that the Barnes Ice Cap had an area-averaged mass loss of 120, 760, and $1000\text{ kg m}^{-2}\text{ a}^{-1}$ for 1970–1984, 1984–2006 and 2004–2006, respectively. These later values compare relatively well with our 1995–2000 and 2000–2005 Barnes Ice Cap estimates of 583 and $722\text{ kg m}^{-2}\text{ a}^{-1}$, respectively, and support our finding that the rate of mass loss from the Barnes Ice Cap has accelerated in recent years.

Putting our results into a more global perspective, Jacob et al. (2012) estimated the total mass loss from glaciers outside of the ice sheets to be $148 \pm 30\text{ Gt a}^{-1}$ for the period January 2003 to December 2010. This period is similar to our September 2003 to August 2011 GRACE estimate, during which the glaciers of Baffin and Bylot Island lost mass at a rate of $23.8 \pm 6.1\text{ Gt a}^{-1}$. This rate of loss represents 16% of total glacier loss outside of Greenland and Antarctica.

6 Conclusions

Between 1963 and 2006 the glaciers of Baffin and Bylot Islands lost ice at rate of $11.1 \pm 3.4\text{ Gt a}^{-1}$ ($271 \pm 84\text{ kg m}^{-2}\text{ a}^{-1}$) increasing to $23.8 \pm 6.1\text{ Gt a}^{-1}$ ($581 \pm 149\text{ kg m}^{-2}\text{ a}^{-1}$) for the period 2003 to 2011. The doubling of the rate of mass loss is attributed to higher temperatures in summer with little change in annual precipitation. In total, between 1963 and 2011, the glaciers of Baffin and Bylot Islands contributed 1.7 mm to the world's oceans. Summer temperatures accounted for 68–98% of the variance in the rate of mass change, to which the Barnes Ice Cap was found to be 1.7 times more sensitive than either the Penny Ice Cap or the region as a whole. The heightened sensitivity of the Barnes Ice Cap is the result of a hypsometry that is skewed towards lower elevations.

Results for the Barnes Ice Cap clearly indicate an acceleration in the rate of mass loss in recent years, which can be

attributed to increases in summer temperature. Results for the Penny Ice Cap also show accelerated losses, but data coverage is not as good as for the Barnes Ice Cap. The good spatial coverage of the SPOT-CDED differencing reveals complex patterns of elevation change for the Barnes Ice Cap and Bylot Island glaciers. Between 2005 and 2011 the Barnes Ice Cap lost ice at an area averaged rate of $1060 \pm 60\text{ kg m}^{-2}\text{ a}^{-1}$ with enhanced elevation lowering in places where the ice cap abuts proglacial lakes. There are also signs of continued “local creep slump” of the ice cap's southwest lobe. For Bylot Island, the SPOT-CDED differencing reveals a complex pattern of valley-glacier elevation change. Under similar climatic forcing, neighboring valley glaciers show markedly different responses over the past 29 years with one of the glaciers experiencing terminus advance (D78) while the neighboring glaciers retreat.

In agreement with other recent studies (Nuth et al., 2010; Käab et al., 2012), our work demonstrates that, with appropriate corrections, regional mass losses can be adequately determined from discontinuous measurements of elevation change. This suggests that the methods used here can potentially be applied to other glaciated areas with poor coverage of elevation data (i.e. use of ICESat and CryoSat at lower latitudes). That said, we find large uncertainties in the extrapolation of ATM elevation change profiles when estimating regional glacier volume changes.

Appendix A

Validation of SPOT DEM using ICESat data is provided in Table A1, and a detailed comparison of CDED with ICESat and SPOT elevations is provided in Table A2. Elevation differencing workflows are provided in Fig. A1 through A3. Locations of ICESat elevations used in the study are provided in Fig. A4, and glacier hypsometry for select regions is provided in Fig. A5.

Table A1. ICESat validation and filtering of SPOT DEMs over glacier-free ground (grd) and over glacier ice (ice). C.P. stands for Cumberland Peninsula.

	Acquisition date yyyymmdd	Standard deviation [m]		Mean elevation difference [m] (SPOT – ICESat)		ICESat postings over valid cells		Elevation-dependent bias	Min. acceptable correlation		% cells excluded	
		grd	ice	grd	ice	grd	ice		grd	ice	grd	ice
Barnes_A V1	20081003	2.4	3.2	–12.5	–13.2	6593	1721	no	0	0	54	46
Barnes_A V2	20081003	2.4	3.8	–12.5	–13.4	6514	974	no	0	0	55	66
Barnes_B V1	20100831*	4.9	1.4	1.3	0	1745	499	yes*	75	0	77	16
Barnes_B V2	20100831*	4.8	1.4	1.2	0	2569	499	yes*	20	0	66	17
Bylot V1	20081001	3.4	5.3	–12.4	–11.3	1087	966	no	85	45	74	26
Bylot V2	20081001	3.4	4.6	–12.3	–11.5	1185	914	no	80	5	73	32
Penny V1	20100707*	4.2	10.6	–3.8	–4.6	913	119	yes*	40	65	73	54
Penny V2	20100707*	5.2	14.2	–3.9	–5.2	952	115	yes*	0	45	73	53
C.P. V1	20100310*	2.8	8.6	3	2.4	1911	503	yes*	0	0	61	38
C.P. V2	20100310*	2.9	6.6	3	1.5	1877	388	yes*	0	30	63	49
Baffin N V1	20100719*	4	1.1	4.8	5	2427	187	yes*	65	80	72	37
Baffin N V2	20100719*	4.5	2.9	4.9	5.3	2647	210	yes*	5	0	69	30

* 2010 SPOT DEMs were compared with 2009 ICESat altimetry (last year of operation). Observed elevation-dependent bias is consistent with expected changes in glacier elevations between acquisition dates, so no correction is applied.

Table A2. Comparison of CDED with ICESat and SPOT elevations over ground before and after co-registration and elevation bias corrections. C.P. stands for Cumberland Peninsula.

	Acquisition date	Standard deviation [m]		Mean difference [m] (ICESat/SPOT – CDED)		Acceptable grid cells/postings	Horizontal misalignment [m]
		before	after	before	after		
ICESat	2004–2008	5.1	4.8	–1.1	0.0	176 253	0
Barnes_A V1	2008	5.4	4.9	–14.7	0.0	3 321 646	18
Barnes_A V2	2008	5.3	4.8	–14.7	0.0	3 240 087	18
Barnes_B V1	2010	5.8	5.4	–1.3	0.0	1 812 114	17
Barnes_B V2	2010	5.8	5.3	–1.5	0.0	2 705 195	17
Bylot V1	2008	7.0	5.5	–11.6	0.0	1 115 868	29
Bylot V2	2008	6.7	5.2	–11.7	0.0	1 194 942	29
Penny V1	2010	13.7	12.7	–6.3	0.0	2 077 098	8
Penny V2	2010	11.8	10.8	–6.2	0.0	2 033 309	7
C.P. V1	2010	8.9	8.0	–0.3	0.0	3 150 830	11
C.P. V2	2010	8.0	7.2	–0.4	0.0	2 991 024	11
Baffin N V1	2010	9.6	8.3	2.7	0.0	1 440 445	14
Baffin N V2	2010	9.1	7.8	2.9	0.0	1 607 803	14

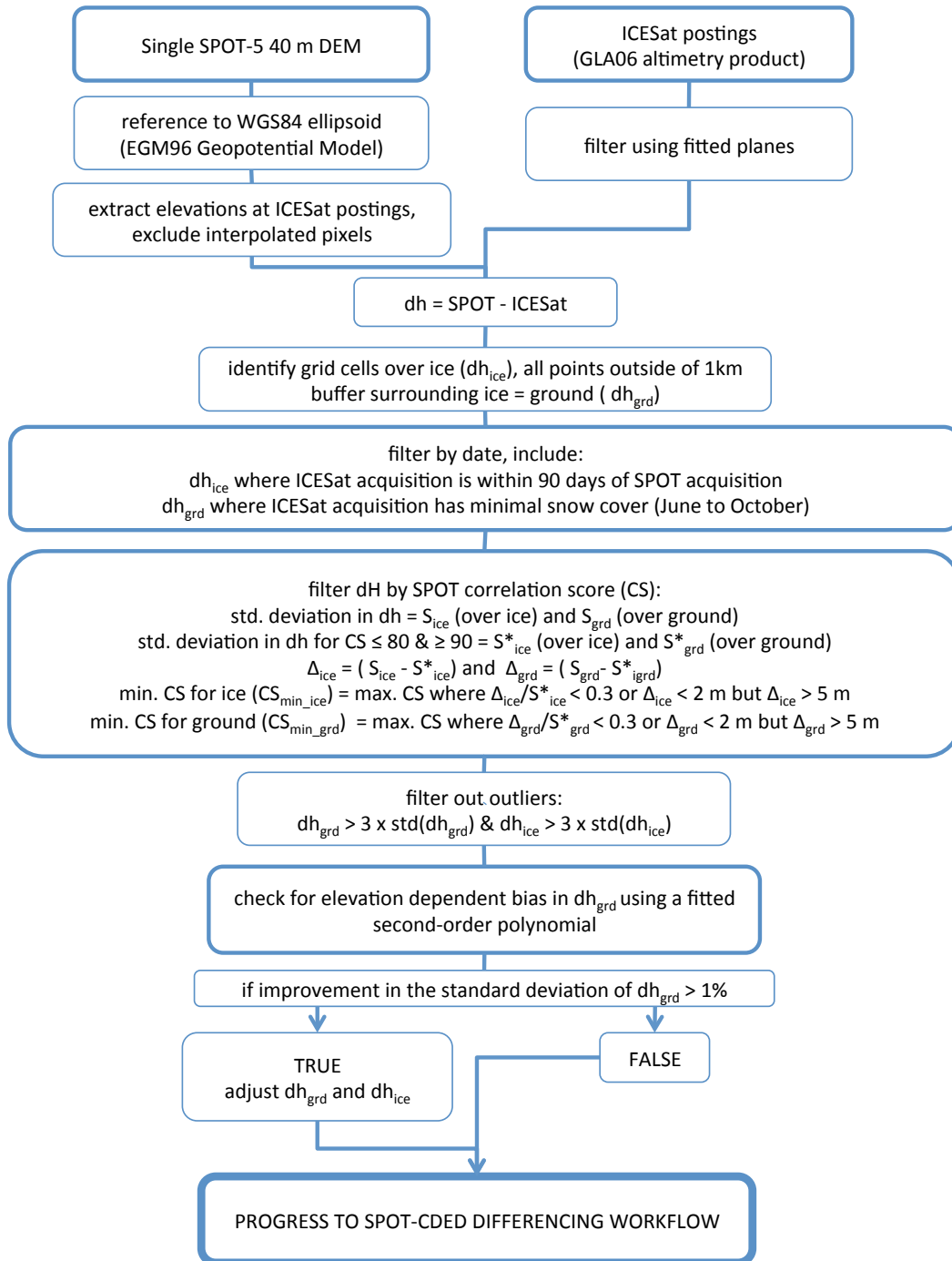


Fig. A1. Workflow for SPOT DEM validation and filtering using ICESat altimetry.

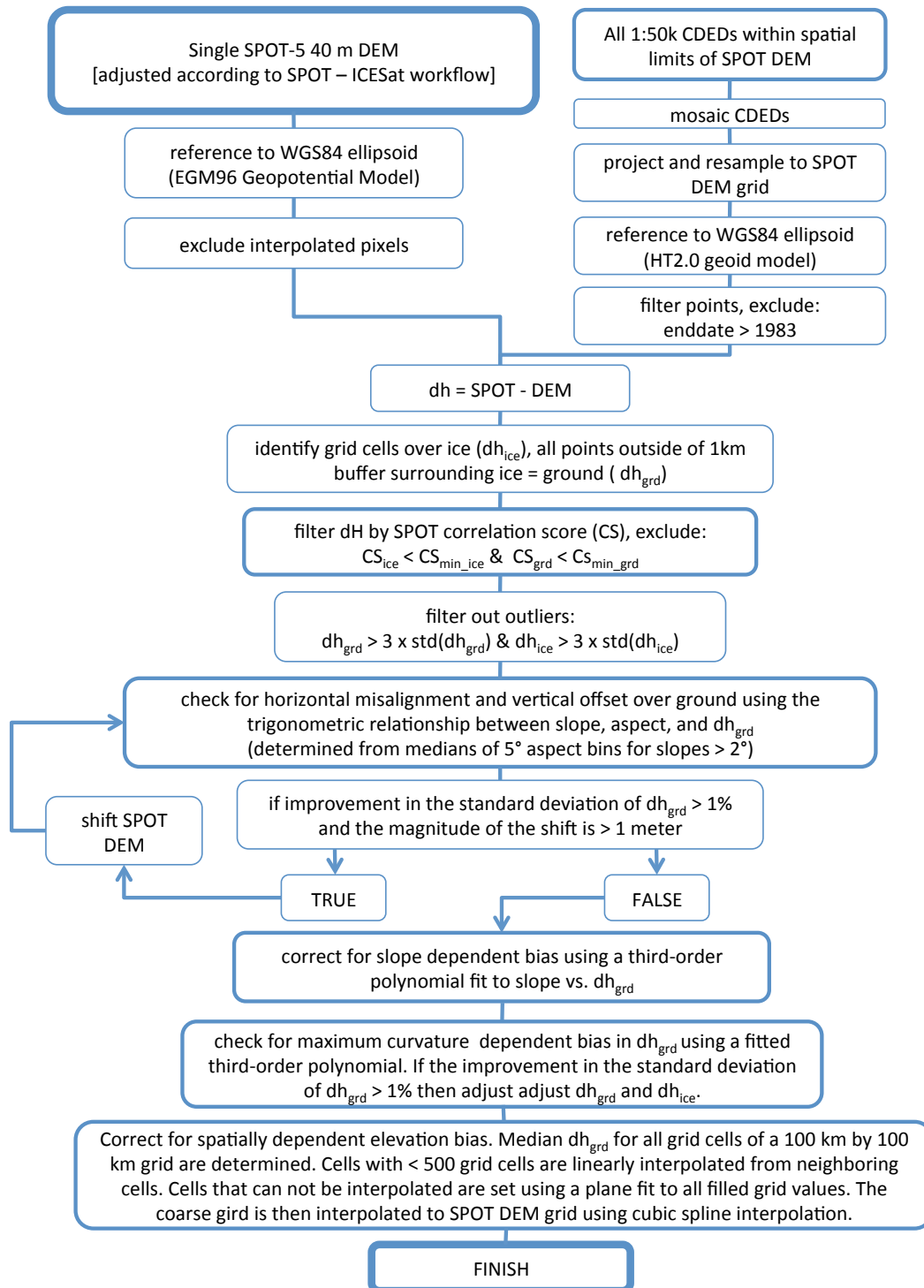


Fig. A2. Workflow for SPOT-CDED differencing.

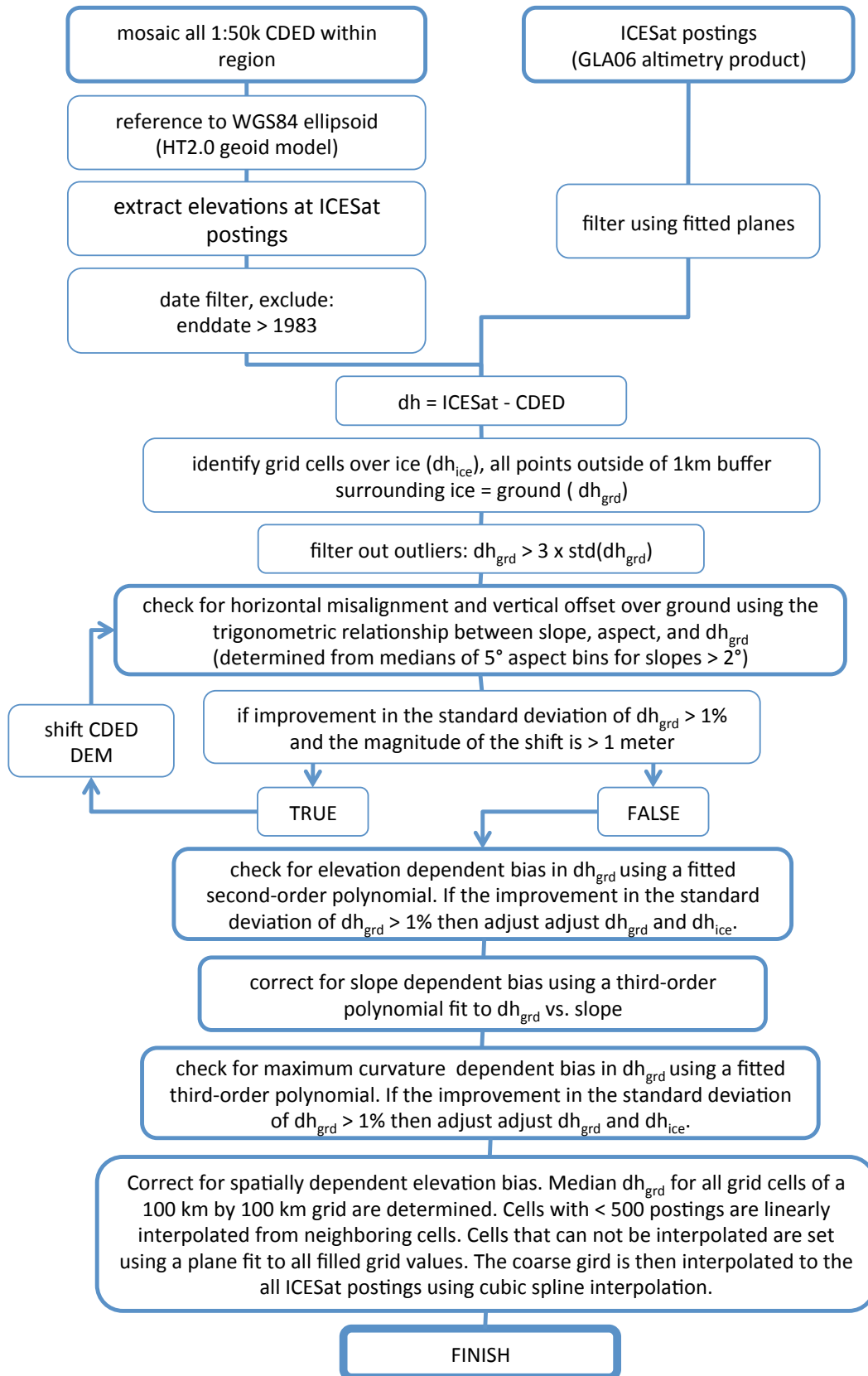


Fig. A3. Workflow for ICESat-CDED differencing.

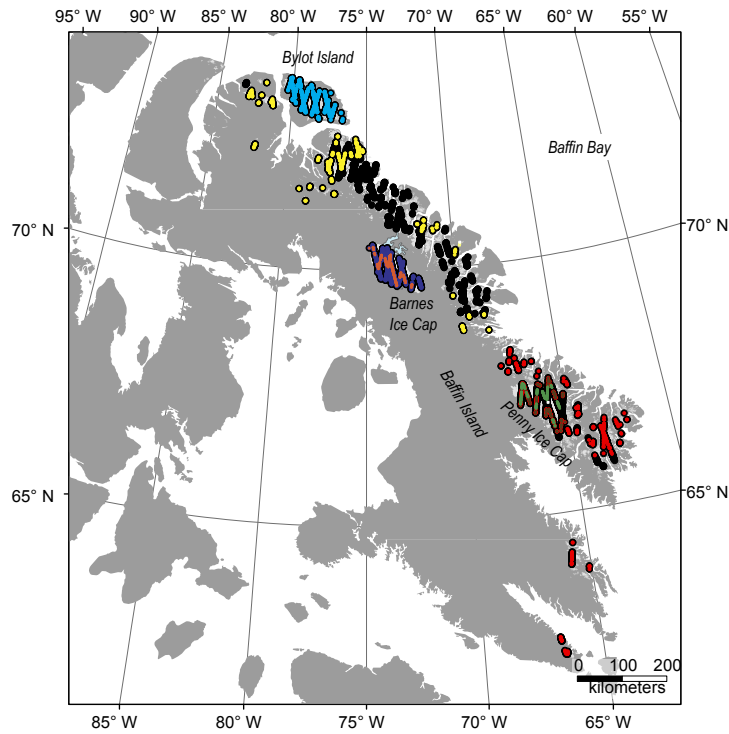


Fig. A4. Locations of ICESat elevations used in study. Underlying black dots (●) show all ICESat points used for ICESat-ICESat estimation of 2003–2009 elevation changes. Cyan (●), yellow (●), blue (●), red (●), and brown (●) dots show the subset of ICESat elevations used for ICESat-CDED differencing for Bylot Island, north Baffin Island, Barnes Ice Cap, south Baffin Island, and the Penny Ice Cap, respectively. Orange (●) and green (●) dots show the subsample of ICESat elevations that are within a 5 km radius of the ATM flight lines and were used to assess the uncertainty in extrapolating ATM-ATM elevation changes to determine regional volume changes.

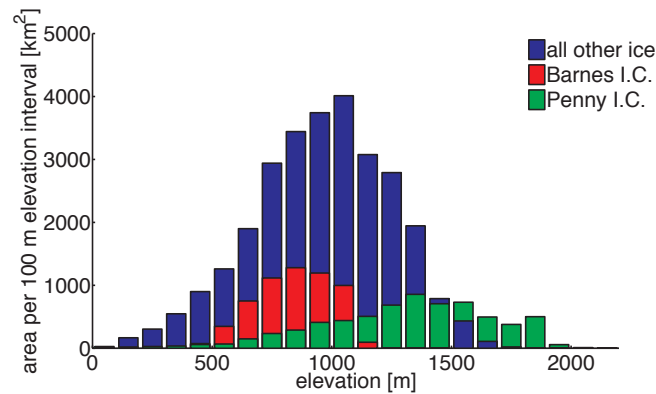


Fig. A5. Glacier hypsometry for the Barnes Ice Cap, Penny Ice Cap, and all remaining glacier ice on Baffin and Bylot Island.

Acknowledgements. We thank A. Beaulieu (Natural Resources Canada) for helping us navigate CDED, E. Berthier (Université de Toulouse) and N. Barrand (British Antarctic Survey) for helping us with the SPOT DEMs, F. Paul (University of Zurich) for generously sharing glacier outlines, and R. Riva and P. Stocchi (TU Delf) for providing glacial isostatic adjustment models. We thank M. Van den Broeke and two anonymous reviewers for their informed and helpful comments. A. Gardner thanks M. Flanner for his support. We thank the many data providers: National Snow and Ice Data Center (ICESat), the Center for Space Research at University of Texas (GRACE), the IPY-SPIRIT project (SPOT-5 DEMs), the US Geological Survey (Landsat imagery), GeoBase (CDED), NOAA/ESRL/PSD (NCEP/NCAR R1), Environment Canada (station data), W. Krabill and the NASA Airborne Topographic Mapping program (pre-IceBridge ATM data) and the National Snow and Ice Data Center (IceBridge ATM data). This work was supported by funding to A. Gardner from NSERC Canada and by funding from NASA Cryospheric Sciences grant NNH07ZDA001N-CRYO to A. Arendt.

Edited by: M. Van den Broeke

References

- Abdalati, W., Krabill, W., Frederick, E., Manizade, S., Martin, C., Sonntag, J., Swift, R., Thomas, R., Yungel, J., and Koerner, R.: Elevation changes of ice caps in the Canadian Arctic Archipelago, *J. Geophys. Res.*, 109, F04007, doi:10.1029/2003JF000045, 2004.
- Andrews, J. T., Holdsworth, G., and Jacobs, J. D.: Glaciers of the Arctic Islands. Glaciers of Baffin Island, USGS USGS Professional Paper 1386-J-1, J162–J198, 2002.
- Bader, H.: Sorge's law of densification of snow on high polar glaciers, *J. Glaciol.*, 2, 319–323, 1954.
- Baird, P. D.: The Baffin Island Expedition, 1950, *Geogr. J.*, 118, 267–277, 1952.
- Beaulieu, A. and Clavet, D.: Accuracy assessment of Canadian Digital Elevation Data using ICESat, *Photogram. Eng. Remote Sensing*, 75, 81–86, 2009.
- Berthier, E., Schiefer, E., Clarke, G. K. C., Menounos, B., and Remy, F.: Contribution of Alaskan glaciers to sea-level rise derived from satellite imagery, *Nature Geosci.*, 3, 92–95, doi:10.1038/ngeo737, 2010.
- Bettadpur, S.: CSR Level-2 Processing Standards Document for Product Release 04, GRACE 327–742, Revision 3.1, The GRACE Project, Center for Space Research, University of Texas at Austin, 2007.
- Clark, P. U., Clague, J. J., Curry, B. B., Dreimanis, A., Hicock, S. R., Miller, G. H., Berger, G. W., Eyles, N., Lamothe, M., Miller, B. B., Mott, R. J., Oldale, R. N., Stea, R. R., Szabo, J. P., Thorleifson, L. H., and Vincent, J. S.: Initiation and development of the Laurentide and Cordilleran Ice Sheets following the last interglaciation, *Quat. Sci. Rev.*, 12, 79–114, 1993.
- Dowdeswell, E. K., Dowdeswell, J. A., and Cawkwell, F.: On the glaciers of Bylot Island, Nunavut, Arctic Canada, *Arc. Antarct. Alp. Res.*, 39, 402–411, 2007.
- Dupont, F., Royer, A., Langlois, A., Gressent, A., Picard, G., Fily, M., Cliche, P., and Chum, M.: Monitoring the melt season length of the Barnes ice cap over the 1979–2010 period using active and passive microwave remote sensing data, *Hydrol. Processes*, 26, 2643–2652, doi:10.1002/hyp.9382, 2012.
- Fisher, D. A., Koerner, R. M., Bourgeois, J. C., Zielinski, G., Wake, C., Hammer, C. U., Clausen, H. B., Gundestrup, N., Johnsen, S., Goto-Azuma, K., Hondoh, T., Blake, E., and Gerasimoff, M.: Penny Ice Cap cores, Baffin Island, Canada, and the Wisconsinan Foxe Dome connection: Two states of Hudson Bay ice cover, *Science*, 279, 692–695, 1998.
- Fisher, D., Zheng, J., Burgess, D., Zdanowicz, C., Kinnard, C., Sharp, M., and Bourgeois, J.: Recent melt rates of Canadian Arctic ice caps are the highest in four millennia, *Global Planet. Change*, 84–85, 3–7, 2012.
- Flanner, M. G. and Zender, C. S.: Linking snowpack microphysics and albedo evolution, *J. Geophys. Res.-Atmos.*, 111, D12208, doi:10.1029/2005JD006834, 2006.
- Fricker, H. A., Borsa, A., Minster, B., Carabajal, C., Quinn, K., and Bills, B.: Assessment of ICESat performance at the Salar de Uyuni, Bolivia, *Geophys. Res. Lett.*, 32, L21S06, doi:10.1029/2005gl023423, 2005.
- Gardelle, J., Berthier, E., and Arnaud, Y.: Slight mass gain of Karakoram glaciers in the early twenty-first century, *Nature Geosci.*, 5, 322–325, doi:10.1038/ngeo1450, 2012a.
- Gardelle, J., Berthier, E., and Arnaud, Y.: Impact of resolution and radar penetration on glacier elevation changes computed from DEM differencing, *J. Glaciol.*, 58, 419–422, doi:10.3189/2012JoG11J175, 2012b.
- Gardner, A. S. and Sharp, M. J.: Sensitivity of net mass balance estimates to near-surface temperature lapse rates when employing the degree-day method to estimate glacier melt, *Ann. Glaciol.*, 50, 80–86, 2009.
- Gardner, A. S. and Sharp, M. J.: A review of snow and ice albedo and the development of a new physically based broadband albedo parameterization, *J. Geophys. Res.*, 115, F01009, doi:10.1029/2009jf001444, 2010.
- Gardner, A. S., Moholdt, G., Wouters, B., Wolken, G. J., Burgess, D. O., Sharp, M. J., Cogley, J. G., Braun, C., and Labine, C.: Sharply increased mass loss from glaciers and ice caps in the Canadian Arctic Archipelago, *Nature*, 473, 357–360, doi:10.1038/nature10089, 2011.
- Holdsworth, G.: Evidence of a surge on Barnes Ice Cap, Baffin Island, *Can. J. Earth Sci.*, 10, 1565–1574, doi:10.1139/e73-148, 1973.
- Holdsworth, G.: Surge activity on the Barnes Ice Cap, *Nature*, 269, 588–590, 1977.
- Holdsworth, G.: Glaciological reconnaissance of an ice core drilling site, Penny Ice Cap, Baffin Island, *J. Glaciol.*, 30, 3–15, 1984.
- Hooke, R. L.: Pleistocene ice at the base of the Barnes Ice Cap, Baffin Island, NWT, Canada, *J. Glaciol.*, 17, 49–59, 1976.
- Hooke, R. L., Johnson, G. W., Brugger, K. A., Hanson, B., and Holdsworth, G.: Changes in mass balance, velocity, and surface profile along a flow line on Barnes Ice Cap, 1970–1984, *Can. J. Earth Sci.*, 24, 1550–1561, 1987.
- Jacob, T., Wahr, J., Pfeffer, W. T., and Swenson, S.: Recent contributions of glaciers and ice caps to sea level rise, *Nature*, 482, 514–518, doi:10.1038/nature10847, 2012.
- Jacobs, J. D., Heron, R., and Luther, J. E.: Recent changes at the northwest margin of the Barnes Ice Cap, Baffin Island, N.W.T., Canada, *Arctic Alpine Res.*, 25, 341–352, doi:10.2307/1551917, 1993.

- Jacobs, J. D., Simms, E. L., and Simms, A.: Recession of the southern part of Barnes Ice Cap, Baffin Island, Canada, between 1961 and 1993, determined from digital mapping of Landsat TM, *J. Glaciol.*, 43, 98–102, 1997.
- Kääb, A., Berthier, E., Nuth, C., Gardelle, J., and Arnaud, Y.: Contrasting patterns of early 21st century glacier mass change in the Hindu Kush – Karakoram – Himalaya, 2012.
- Kalnay, E., Kanamitsu, M., Kistler, R., Collins, W., Deaven, D., Gandin, L., Iredell, M., Saha, S., White, G., Woollen, J., Zhu, Y., Chelliah, M., Ebisuzaki, W., Higgins, W., Janowiak, J., Mo, K. C., Ropelewski, C., Wang, J., Leetmaa, A., Reynolds, R., Jenne, R., and Joseph, D.: The NCEP/NCAR 40-year reanalysis project, *B. Am. Meteorol. Soc.*, 77, 437–471, 1996.
- Korona, J., Berthier, E., Bernard, M., Rémy, F., and Thouvenot, E.: SPIRIT. SPOT 5 stereoscopic survey of Polar Ice: Reference Images and Topographies during the fourth International Polar Year (2007–2009), *ISPRS Journal of Photogrammetry and Remote Sensing*, 64, 204–212, 2009.
- Krabill, W. B.: IceBridge ATM L2 Icessn Elevation, Slope, and Roughness, (May 1995; May to June 2000; May 2005; May 2011). Boulder, Colorado USA: National Snow and Ice Data Center. Digital media, 2011.
- Krabill, W., Abdalati, W., Frederick, E., Manizade, S., Martin, C., Sonntag, J., Swift, R., Thomas, R., Wright, W., and Yungel, J.: Greenland Ice Sheet: High-elevation balance and peripheral thinning, *Science*, 289, 428–430, doi:10.1126/science.289.5478.428, 2000.
- Krabill, W. B., Abdalati, W., Frederick, E. B., Manizade, S. S., Martin, C. F., Sonntag, J. G., Swift, R. N., Thomas, R. H., and Yungel, J. G.: Aircraft laser altimetry measurement of elevation changes of the Greenland Ice Sheet: Technique and accuracy assessment, *J. Geodyn.*, 34, 357–376, doi:10.1016/s0264-3707(02)00040-6, 2002.
- Lambeck, K., Antonioli, F., Purcell, A., and Silenzi, S.: Sea-level change along the Italian coast for the past 10,000 yr, *Quat. Sci. Rev.*, 23, 1567–1598, doi:10.1016/j.quascirev.2004.02.009, 2004.
- Løken, O. and Sagar, R.: Mass balance observations on the Barnes Ice Cap, Baffin Island, Canada, *Int. Assoc. Sci. Hydrol. Publ.*, 79, 282–291, 1967.
- Mekis, E. and Hogg, W. D.: Rehabilitation and analysis of Canadian daily precipitation time series, *Atmos. Ocean*, 37, 53–85, 1999.
- Mekis, E. and Vincent, L. A.: An overview of the second generation adjusted daily precipitation dataset for trend analysis in Canada, *Atmos. Ocean*, 49, 163–177, doi:10.1080/07055900.2011.583910, 2011.
- Moholdt, G., Nuth, C., Hagen, J. O., and Kohler, J.: Recent elevation changes of Svalbard glaciers derived from ICESat laser altimetry, *Remote Sens. Environ.*, 114, 2756–2767, 2010.
- Nuth, C. and Kääb, A.: Co-registration and bias corrections of satellite elevation data sets for quantifying glacier thickness change, *The Cryosphere*, 5, 271–290, doi:10.5194/tc-5-271-2011, 2011.
- Nuth, C., Moholdt, G., Kohler, J., Hagen, J. O., and Kääb, A.: Svalbard glacier elevation changes and contribution to sea level rise, *J. Geophys. Res.*, 115, F01008, doi:10.1029/2008jf001223, 2010.
- Ommanney, C. S. L.: The Canadian glacier inventory, In *Glaciers, Proceedings of Workshop Seminar 1970*, Vancouver, B.C. Ottawa, Ont., 24–25 September 1970, 1971.
- Orvig, S.: The Climate of the ablation period on the Barnes Ice-Cap in 1950, *Geogr. Ann. A*, 33, 166–209, 1951.
- Orvig, S.: Glacial-meteorological observations on icecaps in Baffin Island, *Geogr. Ann. A*, 36, 193–318, 1954.
- Paul, F. and Svoboda, F.: A new glacier inventory on southern Baffin Island, Canada, from ASTER data: II. Data analysis, glacier change and applications, *Ann. Glaciol.*, 50, 22–31, 2009.
- Peltier, W. R.: Global glacial isostasy and the surface of the ice-age Earth: The ICE-5G (VM2) model and GRACE, *Annu. Rev. Earth Planet. Sci.*, 32, 111–149, doi:10.1146/Annurev.Earth.32.082503.144359, 2004.
- Riva, R. E. M., Gunter, B. C., Urban, T. J., Vermeersen, B. L. A., Lindenbergh, R. C., Helsen, M. M., Bamber, J. L., de Wal, R. S. W. V., van den Broeke, M. R., and Schutz, B. E.: Glacial isostatic adjustment over Antarctica from combined ICESat and GRACE satellite data, *Earth Planet. Sci. Lett.*, 288, 516–523, doi:10.1016/J.Epsl.2009.10.013, 2009.
- Rodell, M., Houser, P. R., Jambor, U., Gottschalck, J., Mitchell, K., Meng, C. J., Arsenault, K., Cosgrove, B., Radakovich, J., Bosilovich, M., Entin, J. K., Walker, J. P., Lohmann, D., and Toll, D.: The Global Land Data Assimilation System, *B. Am. Meteorol. Soc.*, 85, 381–394, doi:10.1175/bams-85-3-381, 2004.
- Rolstad, C., Haug, T., and Denby, B.: Spatially integrated geodetic glacier mass balance and its uncertainty based on geostatistical analysis: Application to the Western Svartisen Ice Cap, Norway, *J. Glaciol.*, 55, 666–680, 2009.
- Sagar, R.: Glaciological and climatological studies on the Barnes Ice Cap, 1962–64, *Geographical Bulletin*, 8, 3–47, 1966.
- Schutz, B. E., Zwally, H. J., Shuman, C. A., Hancock, D., and Dimarzio, J. P.: Overview of the ICESat mission, *Geophys. Res. Lett.*, 32, L21S01, doi:10.1029/2005gl024009, 2005.
- Siegfried, M. R., Hawley, R. L., and Burkhart, J. F.: High-resolution ground-based GPS measurements show intercampaign bias in ICESat elevation data near summit, Greenland, *IEEE T. Geosci. Remote*, 49, 3393–3400, 2011.
- Smith, B. E., Fricker, H. A., Joughin, I. R., and Tulaczyk, S.: An inventory of active subglacial lakes in Antarctica detected by ICESat (2003–2008), *J. Glaciol.*, 55, 573–595, 2009.
- Sneed, W. A., Hooke, R. L., and Hamilton, G. S.: Thinning of the south dome of Barnes Ice Cap, Arctic Canada, over the past two decades, *Geology*, 36, 71–74, 2008.
- Swenson, S. and Wahr, J.: Methods for inferring regional surface-mass anomalies from Gravity Recovery and Climate Experiment (GRACE) measurements of time-variable gravity, *J. Geophys. Res.*, 107, 2193, doi:10.1029/2001jb000576, 2002.
- Tushingham, A. M. and Peltier, W. R.: Iice-3G: A new global model of late Pleistocene deglaciation based upon geophysical predictions of post-glacial relative sea level change *J. Geophys. Res.*, 96, 4497–4523, 1991.
- Vincent, L. A., Zhang, X., Bonsal, B. R., and Hogg, W. D.: Homogenization of daily temperatures over Canada, *J. Climate*, 15, 1322–1334, 2002.
- Wahr, J., Molenaar, M., and Bryan, F.: Time variability of the Earth's gravity field: Hydrological and oceanic effects and their possible detection using GRACE, *J. Geophys. Res.*, 103, 30205–30229, doi:10.1029/98JB02844, 1998.
- Ward, W.: Glaciological studies in the Penny Highland, Baffin Island, 1953, *IAHS, General Assembly of Rome*, 4, 297–308, 1954.

- Weaver, R. L.: "Boas" Glacier (Baffin Island, N.W.T., Canada) mass balance for the five budget years 1969 to 1974, *Arctic Alpine Res.*, 7, 279–284, 1975.
- Wouters, B. and Schrama, E. J. O.: Improved accuracy of GRACE gravity solutions through empirical orthogonal function filtering of spherical harmonics, *Geophys. Res. Lett.*, 34, L23711, doi:10.1029/2007gl032098, 2007.
- Wouters, B., Chambers, D., and Schrama, E. J. O.: GRACE observes small-scale mass loss in Greenland, *Geophys. Res. Lett.*, 35, L20501, doi:10.1029/2008GL034816, 2008.
- Zdanowicz, C. M., Fisher, D. A., Clark, I., and Lacelle, D.: An ice-marginal delta O-18 record from Barnes Ice Cap, Baffin Island, Canada, *Ann. Glaciol.*, 35, 145–149, doi:10.3189/172756402781817031, 2002.
- Zdanowicz, C., Smetny-Sowa, A., Fisher, D., Schaffer, N., Copland, L., Eley, J., and Dupont, F.: Summer melt rates on Penny Ice Cap, Baffin Island: Past and recent trends and implications for regional climate, *J. Geophys. Res.*, 117, F02006, doi:10.1029/2011jf002248, 2012.
- Zwally, H. J., Schutz, B., Abdalati, W., Abshire, J., Bentley, C., Brenner, A., Bufton, J., Dezio, J., Hancock, D., Harding, D., Herring, T., Minster, B., Quinn, K., Palm, S., Spinhirne, J., and Thomas, R.: ICESat's laser measurements of polar ice, atmosphere, ocean, and land, *J. Geodyn.*, 34, 405–445, 2002.
- Zwally, H. J., Jun, L., Brenner, A. C., Beckley, M., Cornejo, H. G., DiMarzio, J., Giovinetto, M. B., Neumann, T. A., Robbins, J., and Saba, J. L.: Greenland ice sheet mass balance: Distribution of increased mass loss with climate warming; 2003–07 versus 1992–2002, *J. Glaciol.*, 57, 88–102, 2011a.
- Zwally, H. J., Schutz, R., Bentley, C., Bufton, J., Herring, T., Minster, B., Spinhirne, J., and Thomas, R.: GLAS/ICESat L1B Global Elevation Data V031, 20 February 2003 to 11 October 2009, National Snow and Ice Data Center, Boulder, CO, Digital media, 2011b.